THE UNIVERSITY OF ALBERTA

CORROSION FATIGUE OF STEEL IN HYDROGEN SULPHIDE

by

© RONALD L. PROWSE

SUBMITTED TO THE FACULTY OF GRADUATE STUDIES AND

RESEARCH IN PARTIAL FULFILLMENT OF THE REQUIREMENTS

FOR THE DEGREE OF MASTER OF SCIENCE

IN METALLURGICAL ENGINEERING

DEPARTMENT OF MINING AND METALLURGY

EDMONTON, ALBERTA

SPRING, 1973

To Starr, Michael and Dayle

ABSTRACT

A fatigue loading system was designed to produce zero-tension loading, a slow cycling rate and a square wave loading function. The system was hydraulicly actuated with the desired loading function and cycling rate controlled by a cam-driven four-way flow control valve.

Fatigue tests were performed on a quenched and tempered, medium carbon steel in gaseous environments of air, dry and humid argon, dry and humid hydrogen and dry and humid hydrogen sulphide. The fatigue life was found to decrease in the order of humid hydrogen, humid argon, dry argon, air, dry hydrogen, dry hydrogen sulphide and humid hydrogen sulphide.

An explanation, based on the presence of an oxygen impurity, is advanced to explain the shorter fatigue lives observed in argon than those observed in humid hydrogen.

Dry hydrogen and hydrogen sulphide decreased the fatigue life relative to other environments and caused a change in the mode of fracture as indicated by a fractographic investigation. The decrease in fatigue life and the change in fracture mode is attributed to hydrogen embrittlement mechanism.

ACKNOWLEDGEMENTS

The author is indebted to Dr. M. L. Wayman for providing guidance and encouragement over the span of both my undergraduate and graduate studies.

My thanks to Dr. F. H. Vitovec and Dr. S. A. Bradford for their advice and comments on problems encountered in the research involved in the preparation of this thesis. I would also like to extend my appreciation to Mr. T. Forman, Mr. B. Snider, Mr. G. Chaisson and Mr. R. M. Scott for their able technical assistance.

A special acknowledgement to Mr. W. C. Brockington and the Steel Company of Canada Limited for supplying the sample material used in this project. Also thanks to Dr. M. A. Clegg and Sherrit Gordon Mines Limited for the use of the electron microprobe.

This work was supported by the National Research Council of Canada under Grant number A6074.

TABLE OF CONTENTS

TABLE OF CONTENTS (cont'd)

LIST OF TABLES

T - tables in text

LIST OF FIGURES

LIST OF FIGURES

Figures found in text are labelled with two numbers: the first number indicating chapter, the second number indicating sequence.

I. INTRODUCTION

Hydrogen sulphide has been considered a major problem of the petroleum industry since it threatened the development of the Pincher Creek gas field in southwestern Alberta in 1948. A string of 9% Ni steel tubing from the Walter Marr well number one failed after only six days of production (1). The significance of this failure was reported by the N. A. C. E. Technical Practices Committee 1-G: "The future development of sour-gas condensate fields in Canada and the United States was threatened by the implications of this initial corrosion experience" (2).

As a result of that and subsequent failures attempts have been made to study the mechanism of hydrogen sulphide-induced failure (3, 4, 5). The result has been sets of guidelines for specifying materials for sour service. For example, in 1966 the N. A. C. E. Committee T-1B published report 1F166 (6) entitled, "Sulphide Cracking Resistant Metallic Materials for Valves for Production and Pipeline Service". Even with these and other specifications, failures of such components as tubing, bolts, Christmas tree caps, tool joints, compressor valve springs and sucker rods still occur (7).

For the most part the stresses involved in these failures were considered to be static. It is for this reason that failure attributed to hydrogen sulphide has been labelled stress corrosion cracking or, particularly, sulphide corrosion cracking. However, the stresses in

components such as sucker rods and compressor valve springs are dynamic and therefore a contribution due to metal fatigue cannot be ruled out.

To study the combined effects of corrosion and fatigue a machine has been designed to simulate some of the conditions experienced by a sucker rod. Tests were performed on sucker rod material specifically designed for "sour service": API Grade D 1536 MD steel. Using a slow loading frequency specimens were cycled to failure in air and in dry and humid argon, hydrogen and hydrogen sulphide.

Fractographic studies were performed on the fracture surfaces of specimens fractured in the different environments.

A unique feature of these tests was the slow cyclic loading rate and square stress waveform. The importance of this lies in the enhanced corrosion effect due to the increased time in which the specimen and in particular the crack tip are exposed to the environment.

II. FATIGUE

This chapter deals with the fatigue behaviour of high stacking fault energy materials which have been annealed. Several review articles on fatigue have been published recently (8-12) thus only a condensed summary will be presented here.

2.1 Initial Property Changes

When a material is cyclically loaded at any but the most extreme amplitudes changes in physical and mechanical properties occur rapidly during the first cycles; however, as cycling proceeds the material gradually attains a nearly "saturated" state. Annealed materials respond to cyclic straining by hardening as the total strain accumulates. In the case of high stacking fault energy or "wavy slip" materials such as steel, this occurs during the initial ten percent of the fatigue life.

The microstructural changes that occur are a result of slip. Since grains at a surface or an edge are less constrained than those in the bulk, slip originates in the surface grains and extends into the bulk. Slip is also inhomogeneous which results in the formation of persistent slip bands rather than a completely slipped surface. Once the slip bands have been formed, deformation is then confined to these slip bands. Slip within persistent slip bands, in metals of high stacking fault energy, is very wavy and coarse slip bands with much connecting

cross-slip are observed.

Evidence shows that the structure and properties of persistent slip bands are different from those of the matrix. The bands are markedly softer than the matrix and associated with their development is a steady increase in damping which is not affected by the removal of surface material but may be eliminated by an anneal. Persistent slip bands may also be etched to a depth of at least one mm. beneath the surface. These observations suggest that the formation of persistent slip bands is a bulk effect.

The substructure in the slip bands is dependent on the strain amplitude. At high amplitudes the substructure consists of dislocation cells whose size is determined by the strain amplitude and temperature. Low strain amplitudes produce patches of dislocation dipoles which become denser and more numerous as the amplitude or temperature increases. A mixed structure of cell walls containing dipoles or dipoles grouped into cellular clumps is produced at intermediate amplitudes.

2.2 Fatigue Crack Initiation

Slip in the surface grains is inhomogeneous. As a result, slip bands only partially cover the surface. The degree to which slip occurs in an individual grain depends on the orientation of the grain and the strain amplitude. If the orientation of the grain is such that the

Burgers vector of the operative dislocations lies at some angle to the surface slip steps or grooves (extrusions and intrusions) form as shown schematically in figure 2.1. A taper section, shown in figure 2.2 is conventionally used to magnify the effect.

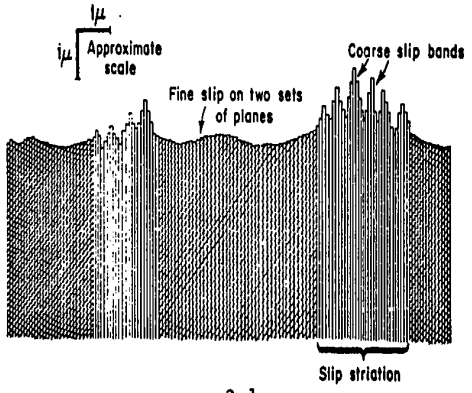

2.1

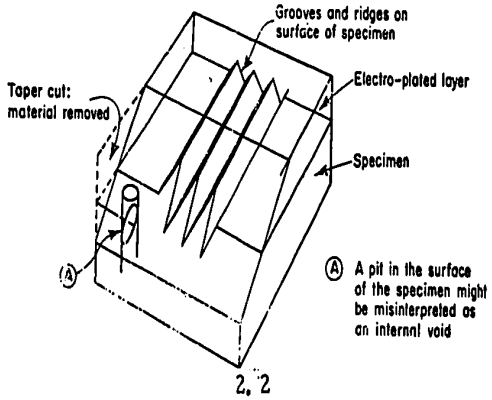

2.2

(taken from P. J. E. Forsyth "Physical Basis of Metal Fatigue")

These features are the result of reverse slip processes and are significant in that there are always detectable slip band cracks at the intrusions (9). The occurrence of the cell structure, which has been observed at a depth of one hundred microns beneath the surface, may also contribute to the initiation of cracks in the persistent slip bands (13).

Since intrusions are primitive notches, it is not surprising that fatigue cracks are observed in the vicinity of these features. Several theories have been proposed to explain the formation of intrusions and extrusions (14-18) but none of them is universally accepted. In annealed material extrusions do not generally appear until saturation.

That a free surface is necessary for crack initiation has been demonstrated by several experiments. If an anodic film is formed on the specimen surface, the formation of slip bands, extrusions and cracks is suppressed as long as the film remains unbroken (19). The fatigue life of such a specimen can thus be extended apparently indefinitely. If slip lines are repeatedly polished away before they can become concentrated in slip bands, or if persistent slip bands are completely machined off, the fatigue life is similarily prolonged.

Fatigue is usually divided into crack initiation and crack propagation stages. Because it is generally accepted that slip bands slowly deepen into crevices and eventually into cracks, this separation of initiation and propagation is rather arbitrary.

2.3 Fatigue Crack Propagation

Observable cracks are usually present well before ten percent of the fatigue life; their behaviour from that point is described as propagation. Propagation occurs in two stages, designated stage I and stage II.

Stage I is a slip plane fracture which occurs by "unslipping" or reverse glide. This is an extension of the initiation process and is controlled by the range of resolved shear stress acting in the slip plane. The crack front may be sharply serrated with the tip acting as a dislocation source. The fracture path, since it follows active slip planes, deviates when it crosses a grain boundary thus giving the fracture surface a faceted appearance but the general fracture plane is one of maximum shear stress.

In most cases the crack grows a short distance into the interior of the specimen and then changes to a stage II crack, growing perpendicular to the direction of maximum tensile stress. The conditions which favour this change are those which prevent easy glide, including high stress amplitude, mean tensile stress, slip plane obstacles such as second phase particles and the growth of the crack into the depths of the specimen where the shear stress to tensile stress ratio is low. Stage II growth is controlled by the value of the maximum principal tensile stress in the region of the crack tip.

As the crack grows the peak tensile stress rises until the amount of plastic deformation is large enough that the characteristic fatigue striations become resolvable on the fracture surface. Each striation results from one stress cycle, the spacing of the striations thus indicating the local crack growth rate.

Striations may be one of two types, brittle or ductile, depending on the environment, stress condition and mechanical properties of the material. Brittle striations lie on crystallographic planes which form facets at an angle to the general fracture plane. They do not normally appear except in corrosive environments. Ductile striations lie on plateaus, the surfaces of which are roughly parallel to the general fracture surface.

As the crack grows longer, the tip stress rises, the striations become more heavily defined and cross slip becomes extensive enough to turn the fracture path back to a plane at 45 degrees to the maximum tensile stress direction. Fracture occurs in the next cycle. This type of fracture is called shear decohesion failure. The stages of crack growth as described above are shown in figure 2. 3 although not in the proportions in which they occur in a specimen.

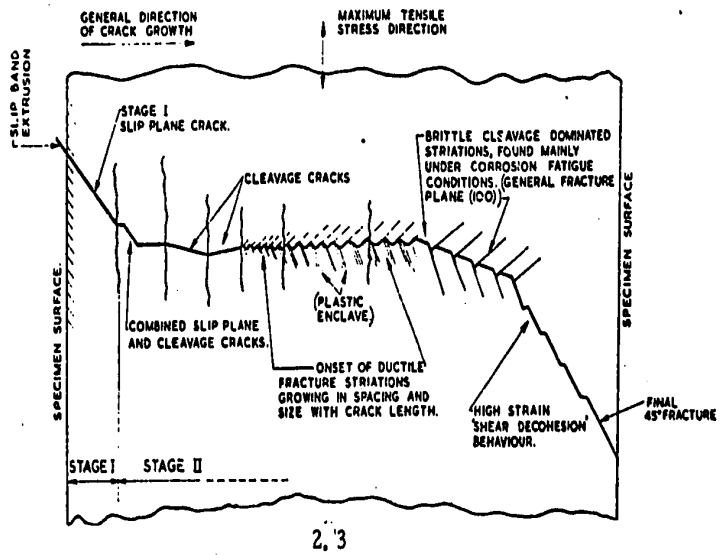

2. 3

(Taken from Acta Met. 11 , 1963)

2.4 Environmental Effects on Fatigue

In constructing a comprehensive view of the combined effects of fatigue and environment, the phenomena of stress corrosion cracking (SCC) and hydrogen assisted cracking (HAC) cannot be neglected. If a material is susceptible to SCC or HAC the addition of a cyclic load will produce fatigue-influenced environmental crack growth. For material systems which are not susceptible to environmental cracking under static load the situation can be described as environment-accelerated fatigue crack growth.

Johnson (20) has proposed a method of distinguishing the two phenomena based on studies of high-strength steels. The proposal is that for yield strengths in excess of 180 ksi, subcritical flaw growth of environmental origin is the major effect and fatigue is less important. At lower strength levels, fatigue and environment-accelerated fatigue become the dominant problems. However Fraser and Eldridge (21) noted sulphide stress corrosion failures in quite soft steel specimens (Ra = 44) when exposed in a highly strained condition to severe environments.

The common denominator between fatigue-influenced environmental crack growth and environmental-accelerated fatigue crack growth is the environment-metal reaction occurring on the clean metal surface at the tip of the fatigue crack. This surface has many interest-

ing properties, the most obvious and important being its catalytic effect on chemical reactions. Because of the importance of the surface a brief review of surface properties and environment-surface interactions is presented. For comprehensive reviews see Latanision and Westwood (22) and Thomas and Thomas (23).

2. 4a Surface Properties

The surface of a crystalline solid has quite different properties than the bulk. The atomic arrangement and lattice spacing, both in the plane of the surface and normal to it may be considerably different than that of atoms in the bulk. Distortion of the surface may occur and it may contain an above average concentration of point and line defects. Solute and vacancy gradients are likely to exist as the surface acts as a sink.

The mechanical behaviour of crystalline materials is largely determined by the generation, motion, and interactions of dislocations. Since it is observed that the presence and condition of the surface can have a major influence on the plastic deformation surface-dislocation interactions are implied. These interactions may be the result of the surface acting as a region in which dislocations are readily formed or as a barrier to the escape of dislocations from within the crystal. Either of these effects would be modified by the presence of surface films and altered further if surface active species were adsorbed.

As previously mentioned slip takes place in the surface grains

and extends into the bulk. Surface removal studies have shown that if this layer of deformed material is removed the original deformation properties are restored. These studies have also lead to the development of three mechanistic models which differ fundamentally in terms of the type and location of dislocation sources. These theories are summarized below.

i. The Debris-Layer Hypothesis

A dislocation-rich debris layer is produced in the surface regions of a plastically deformed crystal by the trapping of some dislocations as they leave the crystal. This debris layer is considered to impede the motion of other dislocations and serves as a barrier against which they pile up. Dislocation pile-ups then produce back stresses on the sources in the bulk of the crystal. Removal of this layer causes recovery of the initial yield stress; the general implication is that work hardening during stage I of a single crystal tensile test is concentrated in the near-surface region. Dissolution of this layer during corrosion fatigue would allow slip to continue as work hardening would not occur. However not all effects can be explained by this model.

ii. The Surface-Source Hypothesis

This model as proposed by Worzula and Robinson (24) involves the generation of dislocations from surface sources. These surface

sources are involved in the yielding of metals. It is reasonable to assume that sources of both the primary and secondary slip systems should be readily activated. This would lead to a preferentially work-hardened layer close to the surface.

The basis for this point of view is that a dislocation line terminating unpinned at the surface but being pinned somewhere in the interior, behaves elastically as a dislocation line in a homogeneous medium which is anchored by the internal pinning point and its image above the surface. The effective length of a Frank-Read source at the surface is then twice its actual length. This implies that only half the stress is required to operate a surface source as compared to a bulk source.

If an adsorbed atom pins the previously unpinned surface end of the source then the stress required to operate the source would increase, effectively increasing the yield stress. Alternatively if dissolution of the metal were occuring new sources would be continually produced as the advancing surface intersected dislocations in the metal.

iii. Near-Surface Sources

Plastic deformation will occur when the applied shear stress is sufficient to activate near-surface sources. Tensile stage I work-hardening of single crystals occurs as a consequence of dislocation loops progressing into the metal from the surface and interacting with the grown-in dislocation forest. The transition to tensile stage II

hardening occurs when the stress concentration at internal barriers is sufficient to activate internal sources on secondary slip systems.

Surface removal before or during loading may or may not decrease the critical resolved shear stress depending on such factors as: the presence of trapped dislocations near the surface, vacancy depletion, solute segregation and the rate of removal of the surface. Continuous surface removal during deformation allows initially activated sources to continue to operate.

For a crystal deforming in the absence of a solvent environment, the surface layers are likely to constitute a barrier to dislocation emergence, leading to trapping and the formation of a debris layer.

The preceeding theories suggest that the effect of environment on mechanical properties is to alter the rate of work-hardening and the ductility as measured by the true stress strain curve. The environment either prevents dislocation emergence from the matrix or prevents the generation of dislocations by the formation of a film. Alternatively, solute atoms can migrate in the near-surface region interacting with mobile dislocations or dislocation sources.

2.4b Surface-Environment Interactions

For a reaction to occur on a surface the following sequence of steps is required.

1. Diffusion of reactants to the surface.
2. Adsorption of the reactants on the surface.
3. Reaction on the surface.
4. Desorption of products.
5. Diffusion of products from the surface.

In general any of these steps may be rate-determining; however, in gaseous reactions steps 1 and 5 are very rarely rate-determining. One of the many previously proposed theories of hydrogen embrittlement by gaseous hydrogen indicates that adsorption is the rate controlling step. The other theories predict that desorption, ie. diffusion of hydrogen into the metal ahead of the crack tip, is rate controlling. The effects of water vapour and oxygen on fatigue crack growth are also considered to be attributable to an adsorption mechanism. As a result it is appropriate to review adsorption mechanisms before discussing the individual theories of the effect of environment on fatigue crack growth.

The first step in adsorption is physical adsorption whereby the adsorbate and the surface of the adsorbent interact by van der Waals forces. These forces are small and the heats of adsorption are low. Also since van der Waals forces are responsible for liquefaction adsorption does not occur at temperatures much above the condensation temperature of the gaseous adsorbate. If the pressure of the gas is near the equilibrium vapour pressure of the liquid adsorbate, then a more

extensive multilayer adsorption occurs.

When the physically adsorbed molecules react chemically with the surface this is termed chemisorption. The energy released upon chemisorption may range from a few to 100 kilocalories per mole. The heat of adsorption of hydrogen on iron is approximately 33 kilocalories per mole (23).

Chemisorption has several possible reaction paths. One adsorbed species may react with another adsorbed species to produce a third product or alternatively an adsorbed molecule can be reduced to two or more products with the surface acting as a catalyst and remaining unchanged. This is termed heterogeneous catalysis and is exemplified by the oxidation of CO on copper oxide. The second possibility is when the metal combines chemically with one of the reactants to form a compound or complex which reacts readily to form products. Formation of iron sulphide is an example of this type of catalysis. Still a third possibility is that the adsorbed species would be adsorbed in the bulk of the metal as when hydrogen is endothermically occluded in iron.

Sites on a surface catalyst differ in their ability to adsorb the reactant molecules. This is demonstrated by the action of catalytic poisons; the effect of strong adsorption of one reactant can be to inhibit or poison the catalyst. Foreign molecules which do not take part in the

reaction can also poison the surface if they are strongly adsorbed. It has been shown that the amount of poison required to stop a reaction is ordinarily significantly smaller than the amount needed to form a mono layer (25).

When adsorption occurs in a capillary, condensation will occur at pressures less than the saturated vapour pressure of the adsorbate. This effect is described by the Kelvin equation:

$$\ln \frac{Po}{P} = \frac{2\gamma\bar{V}}{rRT}$$

where $\bar{V}$ is the molar volume of the liquid, γ is the surface tension, R is the gas constant, T is the absolute temperature, r is the capillary radius, Po is the saturated vapour pressure and P is the vapour pressure of the liquid in the capillary (this derivation is for a cylindrical capillary and does not include a correction for the angle of wetting between the solid and liquid). This equation indicates that as the radius of the capillary is decreased the greater is the lowering of the vapour pressure in the capillary (23). Since a fatigue crack is considered to have the smallest possible tip radius this is a particularly significant phenomena, ie. the saturation vapour pressure near the tip of a fatigue crack is lower than the bulk saturation vapour pressure.

2. 4c Interactions of Hydrogen Sulphide, Water, Oxygen & Hydrogen With Metal

Excluding stress corrosion cracking most environmental effects on fatigue properties are attributed to the presence of either hydrogen or oxygen and theories have been proposed to explain their effects. Before examining these theories the effects of hydrogen sulphide and water will be explained.

i. Hydrogen Sulphide

In 1952 a symposium on sulphide stress corrosion (4) left little doubt that hydrogen sulphide is responsible for the spontaneous failures of steel components in "sour" service. Narrowing the conditions for failure further, Bastien and Amiot (26) showed that embrittlement does not occur in the absence of water or in a nonionizing medium such as benzene.

In their comprehensive study of the problem Sheutz and Robertson (27) compared hydrogen sulphide embrittlement effects with those produced by cathodic hydrogen charging. They also investigated the effects of alloy composition, heat treatment, plastic deformation and chemical environment. Delayed fracture was studied as a function of applied stress, composition and hydrogen concentration. The pertinant conclusions are listed below:

1. The basic cause of failure in sulphide environments is associated

with the absorption of hydrogen. The principal factors determining failure are internal stress, magnitude of applied stress and the hydrogen content.

2. Cold working increases the susceptibility of ferritic steel to failure.

3. Fracture of ferrite or martensite is dependant on stress, hydrogen concentration and time. Above an apparent limiting "endurance stress" fracture is time dependant in the manner of the "static fatigue" of glass and other brittle solids. The endurance stress is inversely proportional to the hydrogen concentration.

4. A trace of sulphide ion in aqueous solution results in a 15-fold increase in the saturation limit of hydrogen absorbed by a nickel steel during cathodic charging in acid.

Warren and Beckman (28) studied the effect of hydrogen sulphide and water on AISI 4140 bolting material with an applied tensile stress. The susceptibility to cracking increased with increasing hardness, increasing applied stress, increasing plastic deformation and decreasing temperature. In the absence of plastic deformation no failures occurred below R_c27 even at stresses near the yield stress. They conclude that the effect of aqueous H_2S can best be explained as hydrogen embrittlement.

In his review of the hydrogen embrittlement phenomena Smialowski (29) quotes Bastien et al. as concluding that sulphide corrosion cracking

and hydrogen embrittlement are equivalent. They also conclude that cold-work increases the susceptibility of steel to fracture and decreases the time to fracture. Smialowski's own conclusion on the subject of sulphide corrosion cracking is "that it is undoubtedly due to the penetration of hydrogen into the metal phase. The presence of the sulphide ion, as a poison of the recombination reaction, evidently causes a high chemical potential of atomic hydrogen on the surface of the steel; the penetration of hydrogen into the bulk of the metal is thereby rendered possible. Since extremely small weight percentages of hydrogen are harmful to the physical properties of steel, a sufficient amount of hydrogen to embrittle the given element may be produced at an insignificant corrosion rate."

The hydrogen sulphide corrosion mechanism is an electrochemical reaction with iron being oxidized at the anode and hydrogen being reduced at the cathode. Sulphur acts to inhibit the recombination of hydrogen and therefore the rate of entry of hydrogen into the metal is increased. Le Boucher (30) believes that the HS^- ion is adsorbed and promotes hydrogen absorption by changing the kinetics of proton discharge. The electrochemical hydrogen sulphide corrosion reaction is shown Appendix A.

Three important features of hydrogen sulphide corrosion that can affect fatigue are the high corrosion rates, precipitation of a corrosion product and liberation of hydrogen.

It has been suggested that a critical corrosion rate exists below which the effect of environment is no longer important to the fatigue resistance of a material (31). The critical corrosion rates of a 0.18% Carbon steel and an AISI type 4140 are reported to be approximately 5 mg. per sq. dm. per day (mdd) and 5.8 mdd respectively (31, 32). Corrosion rates equivalent to 1000 mdd have been measured in aerated aqueous hydrogen sulphide (33).

The precipitation of corrosion products may also prevent the rewelding of the crack faces as the crack closes during the compression or unloading portion of the fatigue cycle. The "prevention of welding" hypothesis is not considered to be the sole cause of the reduced fatigue life in tests where oxide films are formed in the crack. However, it has not been shown that this mechanism is not operative.

Liberation of hydrogen can affect the mechanical properties during fatigue; these mechanisms will be presented in the section dealing with the effects of hydrogen. A fourth possibility is that a combination of two or possibly all three are functioning, perhaps synergistically, and affecting the fatigue mechanism.

ii. Water Vapour

Johnson (34) in reviewing the effects of water and water vapour on the delayed fracture of high strength steels, put forth the following evidence to suggest that the effect of water vapour was one of hydrogen embrittlement.

1. Water-induced brittleness as measured by threshold stress intensity or crack growth rate is comparable in magnitude to that observed with electrolytically-introduced hydrogen contents of less than one part per million.

2. Reversible incubation periods have been reported for both water and hydrogen-induced crack initiation.

3. In both cases a definite critical stress intensity or applied stress, exists below which fracture is not observed.

4. In both cases brittle behaviour is more evident at higher strength levels.

5. A comparison of activation energies for water and hydrogen-induced slow crack growth suggests that hydrogen is the damaging agent in water-induced slow crack growth. This also suggests that the embrittlement mechanism is independant of the source and distribution of hydrogen at the time of stress application.

The agreement between static crack growth rates measured in water and saturated water vapour is striking and has been interpreted to result from water vapour condensation at the crack tip in highly humid environments. At room temperature evidence indicates that condensation occurs at sixty percent relative humidity. A similar saturation behaviour has been observed for moisture-enhanced fatigue crack growth in high strength steels (35). However, capillary condensation has not been demonstrated but only inferred from an equivalence

of crack growth rates.

For a constant humidity the crack growth rate decreases with increasing temperature implying a surface-controlled process connected with water vapour adsorption (13).

The strength of the bond between adsorbed water and the substrate is dependant on the nature of the substrate. Fowkes (36) presents evidence that the bonding of water to metals is mainly by dispersion forces, which are weak. On oxides, on the other hand, the interaction between the water-dipole and the surface field of the oxide is strong and water is tightly bound; the bonding is approximately ten times stronger on an oxide surface than on a metal surface (37).

In studies of the effect of water vapour on the fatigue life of aluminum alloys Bennet (38) showed that hydrogen was evolved during fatigue.

The assumption has been that water and water vapour can supply hydrogen to the surface of steel. This was apparently first shown by Norton (39) and others, more recently (40). The diffusing hydrogen presumably results from the reaction at the steel water interface:

$$3Fe + 4H_2O = Fe_3O_4 + 4H_2$$

Once the initial oxide nucleus had been formed the higher heats of adsorption of water on an oxide would provide increased energy for this reaction. The production of oxide would then continue by a growth process. It is reasonable to assume that a similar reaction occurs

in the case of aluminum. The effect of water, then, is to provide an oxide film which prevents dislocation egress or rewelding of the crack and/or to liberate hydrogen.

iii. Oxygen

Initially oxygen forms an adsorbed mono layer on iron which is more stable than the oxide. As the number of adsorbed layers increase the transformation to the oxide is favoured (41) rather than solution of the oxygen since it is virtually insoluble in iron (42). This film then acts as a barrier to dislocation egress from the crystal.

The mechanism by which films interfere with dislocation emergence from the substrate have been related to the elastic interaction of dislocations with the film-covered surface and to the intimate geometrical and crystallographic relationships between the film and the substrate. A detailed explanation of proposed theories has been presented by Latanision and Westwood (22). As mentioned before the film can also prevent rewelding.

iv. Hydrogen

Adsorption of hydrogen occurs by the breaking of the hydrogen-hydrogen bond followed by chemisorption of hydrogen atoms. Bulk occlusion is then possible. The embrittling effects of hydrogen in steels havebeen studied extensively and several theories have been proposed to explain the phenomena. These theories basically fall into

three groups. The first of these is the "pressure theory" which proposes that embrittlement results from "precipitation" of molecular hydrogen at internal voids and the expansion of these voids by the development of high pressures within them. This theory was first proposed by Zappfe (43) and recently modified by Tetelman (44). The second theory is the "lattice interaction theory" which proposes that hydrogen diffuses under the influence of a stress gradient to regions of high tensile stress within the lattice and interacts with the metal to lower the cohesive strength. This model was proposed by Troiano (45). A third less-widely accepted model, the "stress-sorption theory", was originally proposed by Petch and Stables (46) and has recently been modified by Williams and Nelson (47). Their hypothesis is that surface adsorption and a surface reaction with hydrogen explains gaseous hydrogen embrittlement and embrittlement of hydrogen charged steels.

In the first two theories diffusion of hydrogen through the bulk of the metal is involved. This is often rate determining as indicated by the observed incubation time in delayed failure tests. The tests of Williams and Nelson demonstrate that embrittlement would occur at low hydrogen pressures, 60 torr, and they measured crack growth rates two to five orders of magnitude faster than the maximum expected diffusion rates. They therefore conclude that bulk hydrogen transport cannot be important in the crack-growth process which they observed.

SUMMARY

In summary then, the effects of an aggressive environment may stem from several sources. A surface layer prevents either the generation of dislocations or their emergence from the interior. The result is an increased rate of work hardening or an increased yield stress. An increased yield stress would not necessarily shorten the fatigue life. However, since preferential adsorption occurs adsorption-inhibited slip in one grain would cause a strain concentration resulting in increased slip in an adjacent grain that is not covered by a film.

Aqueous corrosion would remove a work hardened layer increasing the ease of slip if the rate of metal removal is equal to the rate of dislocation generation. If preferential corrosion was taking place slip would be inhomogeneous and strain concentrations would develop.

A third environmental effect would be the bulk occlusion of hydrogen from an external gas environment or from aqueous corrosion and the resultant hydrogen embrittlement.

Combinations of the three mechanisms may also produce a synergistic effect.

It is hoped that this study will provide some evidence as to the mechanism by which an aggressive environment influences the fatigue behaviour of metals.

III. EXPERIMENTAL

3.1 Fatigue Machine

Simulation of service conditions of sucker rods required the construction of a fatigue machine. Due to the time involved in corrosion processes the most important aspect of actual conditions to duplicate is the slow cycling frequency. Another important feature the machine should contain is a stress function in the form of a square wave. The reasons for this will be discussed later. Loading capacity of the machine should exceed 20,000 psi cyclic.

With these requirements and the limitations of economics and time a fatigue loading device was designed. The complete unit is shown in Figure (1). Basically the machine consists of five components:

1. Hydraulic loading system
2. Load frame
3. Load cell
4. Grips
5. Timing mechanism

A detailed discussion of each of these follows.

3.1a Hydraulic Loading System

The hydraulic loading system including motor, pump valves, controls and actuator had previously been assembled by the Alberta

Research Council, Highways Division to simulate traffic loads on soil cement. This system was modified to meet the requirements of this project.

A hydraulic circuit diagram is shown in figure 2. The major modification included the addition of a one-half pint oil accumulator in parallel with the pump. It was felt this would smooth out fluctuations in flow and pressure between the pump and the four-way valve.

To produce the required square wave and slow cycling rate, the original solenoid actuated four-way flow control valve was replaced by a mechanically operated valve. With a mechanically actuated valve the cyclic frequency could be controlled by a belt and pulley system. The valve itself is a Manatrol Colorflow Model 4MD-20-ZM. This valve produces a square loading wave by an on-off regulation of the flow. The time in which a part of the valve was either open or closed could be controlled by the cam mechanism. The result would be that a different amount of time would be spent in one-half of the cycle than the other half. The complete unit is shown in figure 3.

3.1b Load Frame

The load frame was designed to be as accomodating as possible to the present and future projects. Flexibility in specimen length was obtained by the use of threaded support columns. Alignment of the cross heads was performed by adjustment of the individual nuts on each

column. Uniform loading between the nut and the cross head was achieved by machining a spherical surface on one face of the nut and a mating socket on the face of a washer.

Cross head dimensions were taken from a commercial model which had a rated load capacity of 100,000 lbs. static. Construction of the cross heads was by welding followed with a stress relief as residual stresses can be significant in fatigue failures. Following heat treatment load bearing surfaces were machined flat. These surfaces were used as references from which the cross heads were levelled.

3.1c Load Cell

Dimensions and design of the load cell are shown in figure 4. Construction of the load cell was from SPS 245 steel supplied in the annealed condition. The ultimate tensile strength according to manufacturers specifications is 95,000 psi. Estimating the endurance limit as $0.4\sigma_u = 38,000$ psi shows that the required fatigue strength would be achieved, without heat treatment and possible resulting distortion. Increased sensitivity could be obtained by boring the centre hold larger thereby reducing the cross section.

Strain gauge circuitry consisted of two live and two dummy gauges for temperature compensation. The dummy gauges were mounted on a steel block which was held in the centre of the cell by a rubber cork. The other gauges were mounted 180° apart on the reduced sections.

Calibration of the load cell was performed on an Instron Tensile testing machine. Output from the strain gauges was measured on an oscilloscope and recorded. A linear regression analysis was performed on the load versus oscilloscope deflection between (12,000 lbs.) tension and (12,000 lbs.) compression. The analysis yielded the equation:

$$P = 422\ d + 77 \quad \text{tension}$$

$$P = 478\ d - 43 \quad \text{compression}$$

where P = load and d is the oscilloscope deflection measured in centimeters on the 50μ strain scale. The regression coefficient r = 0.9998.

Accuracy of the load measurement is $\pm$ 390 lbs. or 3.2% of the maximum load used in these tests.

3.1d Grips

The grip system is shown in figure 5 Important to this system is the interchangeability of grips which was achieved through the use of hold-down rings. This approach was also the simplest method of attaching grips to the actuator head while leaving some moveability for specimen alignment.

Specimen mounting consisted of loosening the top hold down ring, bolting the specimen in the bottom grip, which was maintained rigid, then bolting in the top grip and finally tightening the top hold down ring to maintain consistency from test to test. The torque on the specimen bolts was 135 foot pounds while 85 foot pounds torque was applied to the

bolts in the hold down ring.

3.1e Timer Mechanism

Fatigue life was recorded by an elapsed time indicator accurate to 0.1 hours. The number of cycles to failure is then the product of cyclic frequency and time to failure.

Failure was ascertained when the increased actuator travel tripped a micro switch which shut off the machine and elapsed time indicator. The circuitry is shown in figure 6

3.2 Testing Procedure

3.2a Specimen Preparation

The steel selected for the tests was A.P.I. Grade D, specifically AISI 1536 sucker rod steel obtained by courtesy of The Steel Company of Canada Ltd. The chemical composition and mechanical properties are listed in Table (1). The material was supplied in 1/4" x 1 1/2" x 3' lengths which had been oil quenched from 1550 F and tempered at 1200 F to a final hardness of 241 BHN. This heat treatment produced a microstructure of finely spherodized carbides and ferrite which is shown in figure 7 A quenched and tempered structure of a hardness not greater than R_c22 (237 BHN) is generally regarded as not susceptible to sulphide stress corrosion (28).

Specimens were machined from the bar stock with the configuration shown in figure (8).

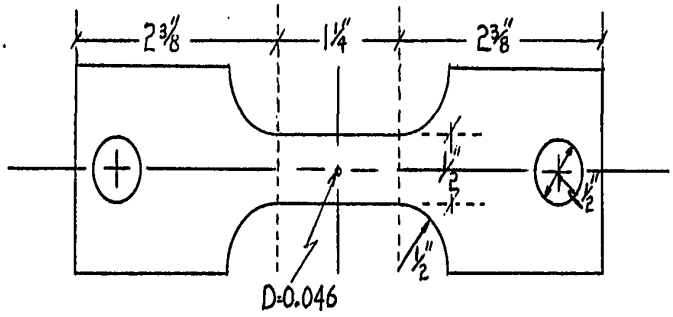

FIGURE 8 SAMPLE CONFIGURATION

The notch was initially drilled to 0.042" and then, after polishing the surface to 320 mesh, reamed to 0.046". Final surface grinding was to 600 mesh to facilitate visual examination of the specimen during cycling. During testing the specimen was monitored with an optical cathetometer in order to observe the propagation of fatigue cracks and the appearance of plastic zones.

3.2b Environment

The environment chamber configuration is shown in figure (9). Production of the rubber seals was accomplished by freezing rubber stoppers in liquid nitrogen, then machining to size. Due to the toxicity of hydrogen sulphide, care had to be taken to prevent leaks. A satisfactory seal was provided by silicone grease. Incorporation of a glass window allowed visual monitoring of the specimen. However, the glass had to be reglued periodically.

Hydrogen sulphide leaks could be detected by filter paper soaked in lead acetate solution. If hydrogen sulphide was present the filter paper turned from white to black. Detection strips were placed liberally around the apparatus. The hydrogen sulphide was exhausted into a fume cabinet.

A positive pressure in the system was maintained by exhausting the gas through approximately 15 mm. of mercury. This also ensured purity as mercury has a low vapour pressure.

Control of the humidity of the gases was exercised in two ways. To produce a gas saturated with water vapour, the gas was bubbled through distilled water maintained at a temperature of 75°C. To dry argon and hydrogen, the gases were passed through a liquid nitrogen cold trap prior to entering the specimen chamber. Hydrogen sulphide was dried by passing the gas through a $CaSO_4$ desicant as a liquid nitrogen cold trap would have condensed the hydrogen sulphide.

The gases were Linde pre-purified hydrogen and argon, and Matheson hydrogen sulphide. Analyses are shown in Table (2).

3.2c Loading Conditions

Loading conditions for the tests were zero-tension, constant load. The load function was a square wave. Cyclic frequency was maintained throughout the tests at 26.4 cycles per minute. This was calculated by recording the number of cycles over a series of twenty

minute time periods and averaging the results.

TABLE 2

GAS COMPOSITIONS

	Argon	Hydrogen	Hydrogen Sulphide Cyl I	Hydrogen Sulphide Cyl III
Argon	remainder	—	—	—
Hydrogen	1 ppm	remainder	—	—
Hydrogen Sulphide	—	—	remainder	remainder
Oxygen	5 ppm	5 ppm	—	—
Nitrogen	10 ppm	5 ppm	—	—
Hydrocarbons	1 ppm	1 ppm	0.1%	0.10%
Water	5 ppm	5 ppm	0.1%	0.15%
Carbon Dioxide	1 ppm	1 ppm	—	1.1%

3.2d Electron Fractography

Specimens were obtained for fractographic analysis by cutting the fatigued specimen perpendicular to the fracture surface at the notch, then parallel to the fracture surface. These specimens were mounted on stages with conducting glue and examined in a Cambridge Stereoscan Mark IV scanning electron microscope.

3.2e Optical Microscopy

Sectioned specimens were polished by conventional techniques then examined on a Zeiss Ultraphot metallograph for such features as surface cracks, and crack branching and their relation to the microstructure.

3.2f X-ray

Powder diffraction patterns of the scale formed on the specimen during fatigue in hydrogen sulphide were obtained on a Philips x-ray diffraction unit using Co radiation and an Fe filter.

3.2g Electron Probe Microanalysis

Electron probe microanalysis was used to confirm the results obtained by x-ray diffraction and to study the possibility of internal diffusion of sulphur into the iron. The studies were performed on a Philips probe using a 30KV accelerating voltage.

IV. RESULTS AND DISCUSSION

This discussion will consist of two parts; the design and construction of the fatigue machine and the results of fatigue tests performed on the machine in inert and aggressive environments. (As the proof of the pudding is in the eating so the results of the fatigue tests are indicative of the performance of the machine.) There are, however, several unique features of the machine that had considerable bearing on the results and these features will be discussed in this light. Following this the results of the fatigue tests will be considered in detail.

4.1 The Machine

By the conclusion of the testing program the machine had operated for almost 400 hours during which the longest continuous run was 37.2 hours. All elements of the machine performed satisfactorily. Only the cycling mechanism showed signs of wear between the steel roller on the valve push rod and the brass cam. Replacement of the brass cam with a hardened steel cam would solve this problem. A further recommendation is the incorporation into the system of an automatic control to shut off the machine in the event of a hydraulic line break which would result in loss of fluid. This would allow the operator to leave the machine for a period of time; in its present condition

continuous monitoring is required.

The grip system is most important in determining the axiality of loading. Examination of test results and specimen fracture surfaces provided evidence of the degree of uniaxial loading. The result of misalignment of the grips is to induce a biaxial state of stress in the specimen thereby decreasing the fatigue life. Since the degree of scatter was not large, either all specimens were aligned or all were misaligned. Examination of the macroscopic fracture surfaces showed that generally the crack front was parallel to the notch. Infrequently a crack would initiate on one side of the notch before it was detected on the other side. When initiation did occur on the slow side, the crack appeared to propagate faster so that at fracture both cracks were approximately the same length. One sided initiation or the fact that all crack fronts did not grow parallel to the notch may be attributed to the statistical nature of fatigue.

Of the four components comprising the machine, the cycling device provided one unusual feature, a square wave form, which helped to clarify certain environmental effects. It has been suggested (20) that environment induced cracks propagate primarily during the maximum load period of the cycle, whereas pure fatigue cracks propagate primarily during the increasing load period. To verify it was desirable to produce a square wave loading function. A photograph of a load cycle

taken with an oscilloscope camera is shown in figure 10. Several things are apparent from this photograph. On application of the load thereis aregion of increasing loading rate, I, a constant loading rate region, II, the constant load region, III, period of decreasing load, IV, and finally a period of zero load, V. The asymmetry of the wave is a result of the characteristics of the four-way valve.

The relative time spent in regions I and II is a function of the maximum load. As the maximum load was increased, the time spent in region I decreased and the time in region II increased. Table 3 shows loading rates corresponding to the minimum and maximum loads used in this study.

TABLE 3

LOADING RATES

Load lbs.	Strain rate in./in./sec. I	II	Cross head Displacement rate in./sec.
4,800	.002	.013	.002
12,000	.025	.036	.007

These results were obtained by measuring the strains in a one inch gauge length of an unnotched specimen. The strain concentrating effect of the circular notch used in specimens in this program was enough to produce yielding, therefore the strain rates in the material adjacent to

the notch were higher than is indicated by the preceeding table.

The high loading rates resulted in a slight overshoot of the maximum load. This situation was desirable in that a sharp boundary existed between the region of rising load and the region of maximum load. The overshoot in no case constituted more than 3% of the maximum load. Effects of loading rates and wave form on specimens fatigued in environments of varying degrees of severity will be discussed later.

4.2 Fatigue Testing

Results of the fatigue tests are tabulated in Table 4. The results are also presented graphically in figures 11 and 12, which are plots of the stress amplitude versus the log of the number of cycles to failure. Figure 11 shows the results of tests performed in dry and humid argon, in humid hydrogen and in air; while figure 12 shows the results of tests in humid hydrogen, dry hydrogen and dry and humid hydrogen sulphide atmospheres.

An attempt was made to distinguish the effects of aggressive atmospheres on the initiation stage from their effects on crack propagation rates; however, the formation of a black sulphide scale on the surfaces of samples tested in moist hydrogen sulphide made early crack detection (by surface observation) impossible. Difficulties were also encountered in detecting small cracks in the other environments with the result that appreciable scatter in the crack initiation times was observed.

Metallographic examination of sectioned specimens indicated that the aggressive environments did not produce a noticeable increase in the number of surface cracks or in the amount of crack branching which occurred during the tests. Figures 13 and 14 show branching and surface cracks which occurred in humid argon and humid hydrogen environments, respectively. Similar effects were observed in other environments.

Since the frequency with which surface cracks formed was roughly independent of environment the implication is that the environment does not have a marked effect on the ease of crack initiation, and that therefore the major effect of the environment is on the rate of crack propagation. However this is not conclusive and the results of these tests will therefore be discussed as the effect of environment on fatigue life.

i. Tests in Dry and Humid Argon, Humid Hydrogen and Air

Examination of figure 11 shows that fatigue lives in dry argon, humid argon and air are the same and are substantially shorter than in humid hydrogen. The explanation is believed to lie in the adsorption behaviour of the various atoms and molecules on the clean metal surface exposed to the environment during fatigue, and in the capillary effect of the fatigue crack.

In a single component gas phase either oxygen or hydrogen will chemisorb on iron, whereas water will form a weaker bond due to physical adsorption. It would be reasonable to assume that chemisorption occurs in preference to physical adsorption because of the larger decrease in free energy associated with chemisorption. Similar reasoning would indicate that oxygen should adsorb in preference to hydrogen. Evidence to support this has been supplied by Hayward and Trapnell (48), who used low-energy electron-diffraction on nickel to show that oxygen adsorbed preferentially to hydrogen and

that oxygen was displaced by hydrogen when the oxygen supply was removed.

In water-hydrogen, water-argon and water-oxygen two component gas systems, the high critical temperatures and near saturation pressures of water would cause moisture to condense in a crack due to the capillary effect. Condensation could occur after an adsorbed layer of other gases had formed; however, once condensation had occurred direct contact of the gaseous environment with the metal surface is no longer possible. Therefore, it would be expected that water would act as a shield to isolate, at least partly, the metal surface from the atmosphere.

Previous fatigue studies have shown that water does in fact protect a specimen from a gaseous environment. Spitzig et al. (49) showed that crack propagation rates for an 18% Ni (250) Maraging Steel in humid hydrogen and dry and humid argon were the same. Crack propagation rates in dry hydrogen were approximately three times faster than in humid hydrogen indicating that moisture can protect the metal from hydrogen. Similarily, Duquette and Uhlig (32) showed that moisture will partially protect samples of 0.18% Carbon steel fatigued in oxygen. The fatigue life of samples tested in humid oxygen was longer than those fatigued in dry oxygen but shorter than lives in dry and humid argon.

These results show that water in the environment does limit the amount of hydrogen or oxygen reaching the crack surface. A possible explanation is that since the solubilities of hydrogen and oxygen in water are low (0.85 cm^3 per 100 cm^3 H_2O and 2.46 cm^3 per 100 cm^3 H_2O respectively), (50) the rate controlling step in the gas-metal reaction may be the solution of the gas in the condensed water layer.

A complete explanation of the fatigue results requires the hypothesis that the presence of oxygen has a detrimental effect on the fatigue life. This can arise from the formation of an oxide film which may change the rate of work-hardening, the yield stress and/or prevent rewelding of the crack faces as previously mentioned.

In the present case the fatigue lives in dry and humid argon are the same as in air and are shorter than the fatigue lives in humid hydrogen. This can be explained by the presence of oxygen in the argon.

It is believed that oxygen entered the system by permeating through the tygon tubing used in transporting the gas to and from the specimen chamber as well as being an impurity in the gas. Grosskreutz and Bowles (51) point out that during fatigue tests at 10^{-6} torr a monolayer of oxygen can form on the surface in about one second. The presence of oxygen in the argon environment explains the similarity between the dry argon and air curves. (Fig. 11)

Comparison of the tests in dry and humid argon shows the effects of water to be significantly smaller than the effects of oxygen. Electro-

chemical corrosion of the iron by oxygen can take place in a condensed water film producing hydrogen and an oxide film. This possibility existed in the humid argon environment. Since water was not present in the dry argon and since the fatigue lives are equal in dry and humid argon electrochemical corrosion may be discounted as the cause of the reduced fatigue lives (relative to humid hydrogen) in dry argon. An explanation of why water does not completely shield the metal from oxygen arises from studies on water-metal and water-oxide bond strengths. Fowkes (36) presents evidence that the bonding of water to metals is mainly by weak dispersion forces. On oxides, on the other hand, the interaction between the water dipole and the surface field of the oxide is strong and water is tightly bound (37). As stated earlier oxygen will adsorb on a metal in preference to water and form an oxide. The water molecules will adsorb more strongly on the oxide than on the metal and will not migrate off the oxide onto the metal surface. Thus water would not be protecting the freshly exposed metal at the crack tip from oxygen.

If oxygen was entering the system from an external source it would be expected to affect the results of tests in humid hydrogen; however, there is not a large effect. A reasonable explanation is that the hydrogen continually reduces any oxide film that is forming or reacts directly with oxygen on the metal surface to form water. Therefore the fatigue life in humid hydrogen would be increased

(relative to the other environments) because of the absence of an oxide film.

Hydrogen may have been entering the steel either from an electrochemical corrosion process or from gas dissolved in the condensed water layer in the crack. The lack of a reduction in fatigue life due to hydrogen may be attributed to the type of steel used. Snape (52) and Bastien (53) have determined that the microstructure and composition of steel most resistant to hydrogen attack are the types used in these tests; however, no steel is considered completely resistant to hydrogen. It is therefore reasonable to assume that in the humid hydrogen and humid air atmospheres hydrogen did not occlude in the metal in large enough concentrations to produce embrittlement.

To summarize, the fatigue lives in dry and humid argon and in air are believed to be the same because of oxygen impurity which resulted in the formation of an oxide film. In the humid hydrogen atmosphere it is believed that the hydrogen prevented the formation of an oxide film and thus the fatigue life was longer.

ii. Tests in Hydrogen and Hydrogen Sulphide

The effects of hydrogen and hydrogen sulphide are shown in figure 12. As explained previously humid hydrogen represents an environment where the effects of hydrogen are small. Comparison of the fatigue life in dry hydrogen to the life in air shows that dry hydrogen does shorten the fatigue life relative to air. The implication is

that a larger amount of hydrogen was reaching the metal in the dry hydrogen atmosphere than in the humid hydrogen atmosphere and that this larger concentration was sufficient to be detrimental to the fatigue properties of the metal.

As mentioned earlier, the effect of sulphur is to increase the amount of hydrogen entering the steel. This implies that a larger amount of hydrogen would enter the steel during tests in hydrogen sulphide.

Despite the fact that dry hydrogen sulphide is non-corrosive to iron at room temperature (10), these results indicate a shorter fatigue life in dry hydrogen sulphide than in dry hydrogen. This can be explained by the formation of water in the dry hydrogen sulphide as a consequence of the presence of oxygen. Oxidation of the dry hydrogen sulphide could form the initial water according to the Claus Reaction:

$$H_2S + 3/2\,O_2 \longrightarrow H_2O + SO_2$$

$$SO_2 + 2H_2S \longrightarrow 3S + 2H_2O$$

Once this water is present, hydrogen sulphide can dissolve (the solubility in warm water is 186 cm^3 H_2S per 100 cm^3 H_2O (50) and electrochemical corrosion can begin. The corrosion reaction produces iron sulphide and releases hydrogen. The presence of sulphur or the HS- ion on the surface then inhibits the recombination of hydrogen and hydrogen atoms enter the steel. The presence of hydrogen can increase crack propagation rates by hydrogen embrittlement as explained below.

The similarity of the fatigue lives of specimens cycled in dry and humid hydrogen sulphide at the same stress level indicate the afore-mentioned process may be operative. Water may also have been present as an impurity in the gas in large enough concentrations to affect the fatigue life.

During tests in wet hydrogen sulphide a black scale formed on the specimens and on the crack surfaces. Samples tested in "dry" hydrogen sulphide also exhibited a slight discolouration. The results of an x-ray powder diffraction analysis on the scale are shown in Table 5.

Angle O	d spacing
10.3	5.0025
16.7	3.1126
17.62	2.9549
22.87	2.3015
29.22	1.8023
29.76	1.8020

All peaks except the one at 16.7° correspond to the peaks listed in the ASTM, powder diffraction file for Mackinawite, FeS, (card no.15-0037).

An iron sulphide scale is not considered adherent except at high pH as explained in Appendix A. Examination of Figure 15 shows that the scale consists of tiny spherules of iron which would not appear to be adherent. Therefore the scale formed during fatigue in hydrogen sulphide would not produce the same effect as would an adherent oxide, ie. it would not lead to the formation of a work-hardened surface layer by the prevention of dislocation emergence, but might prevent rewelding,

thus affecting crack propagation rather than initiation. Evidence presented below however, indicates that there is little if any effect on crack propagation. Electron probe microanalysis showed that sulphur was present only on the surface and had not diffused into the bulk of the steel. Therefore it is reasonable to assume that sulphur did not affect the fatigue mechanism by interaction with dislocations and dislocation sources.

Observations to this point indicate that saturated hydrogen sulphide and dry hydrogen shorten the fatigue life relative to air and humid hydrogen. The presence of hydrogen sulphide results in electrochemical corrosion of the steel, precipitation of iron sulphide and the release of hydrogen.

A clue to the effect of the hydrogen on the decreased fatigue life is given by the shape of the load function. Analysis of the loading conditions show that the effects of hydrogen could not have been manifest during the stage II part of the load cycle. It has been previously shown that at strain rates exceeding 10^{-2} sec^{-1}, very little hydrogen embrittlement phenomena exists. The strain rate at which maximum embrittlement exists is approximately 10^{-3} sec^{-1} (53). Therefore hydrogen embrittlement may have occurred during stage I or stage III of the load cycle. However only low loads were applied during stage I, therefore it is reasonable that hydrogen embrittlement occurred during stage III, the constant load part of the cycle.

The preceeding explanation provides a means of evaluating the process which causes the decrease in the fatigue life in hydrogen sulphide. If hydrogen embrittlement is responsible for the decreased fatigue life in hydrogen sulphide then the fracture surface of samples fatigue in dry hydrogen and in hydrogen sulphide should be similar. If on the other hand, corrosion is responsible, the high corrosion rate in H_2S would remove surface features and the fracture surfaces would look different.

iii. Fractography

Fractographic results support the hypothesis that hydrogen embrittlement is responsible for the decreased fatigue life in hydrogen sulphide. Fractographic techniques have recently been reviewed by Ryder (54) and others (55).

The significant feature of specimen surfaces fatigued in various environments is the difference in the amount of plastic deformation as manifest in the roughness of the fatigue fracture surfaces. Figures 15 and 16 show the surface of specimens fatigued in hydrogen sulphide. Large flat areas are noticeable indicating possible cleavage or quasic-leavage. The surfaces of specimens fatigued in dry hydrogen (Fig. 17) are similar to the fracture surfaces produced in hydrogen sulphide. Comparison of these with surfaces of samples fatigued in humid hydrogen (Fig. 18) shows the relatively small amount of plastic deformation produced by the hydrogen sulphide. Comparison of Figures 18 and 19

indicates a similar amount of plasticity was produced in samples fatigued in humid hydrogen and humid argon.

Thus fractographic evidence shows that hydrogen sulphide produces the same surface morphology as dry hydrogen. Fatigue crack growth in both of these environments occurs with less plastic deformation than in either humid hydrogen or humid argon.

The similarity of fracture surfaces of specimens tested in dry hydrogen and in hydrogen sulphide suggests that the high corrosion rate of the hydrogen sulphide corrosion reaction is not affecting the crack propagation. The decreased life in hydrogen sulphide relative to hydrogen is therefore probably the result of the higher hydrogen concentrations entering the metal due to the poisoning effect of the sulphur in the corrosion products.

With the fractographic evidence indicating a difference in the fracture mechanisms of specimens tested in argon, air and humid hydrogen as compared to hydrogen sulphide and dry hydrogen it becomes more evident that hydrogen embrittlement in this case is a bulk effect. This work then supports the theories of bulk metal-hydrogen interactions and is in opposition to the stress-sorption theory of hydrogen embrittlement. A mechanism by which hydrogen could cause a change in fracture mode and the fracture surface appearance by means of a surface reaction has not been put forth to this time and is most difficult to imagine.

In summary, hydrogen and hydrogen sulphide shorten the fatigue life relative to air and humid hydrogen. Corrosion due to hydrogen sulphide is electrochemical and an iron sulphide is the corrosion product. Fractographic evidence indicates that the removal of material by corrosion at the crack tip is not responsible for the decreased fatigue life in hydrogen sulphide. Fractography does show that specimens fatigued in hydrogen sulphide and in hydrogen have similar fracture surfaces, indicating that hydrogen is responsible for the reduced fatigue life. Because of the poisoning effects of corrosion products from the hydrogen sulphide corrosion reaction more hydrogen is entering the steel from the hydrogen sulphide environment than from the dry hydrogen environment. This indicates that the hydrogen embrittlement effect increases with increasing concentration of hydrogen in the steel. Furthermore, the mode of deformation indicates that hydrogen embrittlement is a bulk effect.

V. CONCLUSIONS

1. A fatigue testing system to produce zero-tension loading in a square-wave loading-mode was designed, constructed and found to function satisfactorily.

2. Decreases were observed in the fatigue life of A. P. I. Grade D 1536 MD steel relative to the fatigue life in a humid hydrogen environment. These decreases, in the case of air and dry and humid argon atmospheres are believed to be due to the presence of an oxygen impurity.

3. Dry hydrogen and hydrogen sulphide environments produce a larger decrease in fatigue life than environments in which oxygen was affecting the fatigue life. The decrease in the fatigue life of steel tested in dry hydrogen and hydrogen sulphide atmospheres is believed to be due to a hydrogen embrittlement mechanism occurring in the bulk of the material. The presence of hydrogen produced a change in the fracture mode. Inhibition of the hydrogen recombination reaction by hydrogen sulphide corrosion products caused a greater amount of hydrogen to enter the steel and a decreased fatigue life in hydrogen sulphide environments was observed relative to dry hydrogen environments.

4. The maximum hardness of $R_c 23$ and a microstructure consisting of spherodized carbides in ferrite does not guarantee immunity from hydrogen sulphide-induced failure when the material is subjected to fatigue loading.

REFERENCES

1. Vollmer, L. W., Corrosion 8, 1952, pp. 326.

2. Report of Technical Practices Committee 1-G, Corrosion 8, 1952.

3. Chittum, J. F., Materials Protection, April, 1968, pp. 30.

4. Symposium on Sulphide Stress Corrosion, Corrosion 8, 1952, pp. 326.

5. Hudgins, C. M., Glasson, R. L., Mehdizadeh, and Rosborough, W. M., Corrosion 22, 1966, pp. 238.

6. National Association Corrosion Engineers Publication 1F-166, Materials Protection 5, 1966, pp. 81.

7. Private Communication, Shell Oil Limited, Calgary, Alberta.

8. Fatigue-An Interdisciplinary Approach, Burke, J. J., Reed, N. L., Weiss, V., eds. Syracuse Univ. Press, 1964.

9. Forsyth, P. J. E., Physical Basis of Metal Fatigue, American Elsevier, 1969, New York.

10. Fatigue Crack Propagation ASTM STP 415, American Society Testing and Materials, 1966.

11. Ham, R. K., Can. Met. Quart. 5 (3), 1967.

12. Forrest, P. G., "Fatigue of Metals", Addison Wesley, London, 1962.

13. Wayman, M. L., M. Sc. Thesis, McMaster University, Hamilton, 1966, pp. 21.

14. Mott, N. F., Proc. Roy. Soc., A242, (1), 1957.

15. Mott, N. F., Acta Met. 6, 1958, p. 195.

16. Cottrell, A. H., and Hull, D., Proc. Roy. Soc. A242, 1957, pp. 211.

17. Nagai, R., J. Phys. Soc. Japan 14, 1959, pp. 1252.

18. Forsyth, P. J. E., Crack Prop. Symposium, Cranfield, 1961.

19. Alden, T. H., and Backofen, W. A., Trans. A. I. M. E., 215, 1959, p. 510.

20. Johnson, H. H., Fracture III, Chapter 12, Leibowitz, ed.

21. Fraser, J. P. and Eldredge, G. G., Corrosion 14, 1958, 524t.

22. Latanision, R. M. and Westwood, A. R. C., "Advances in Corrosion Science and Technology I", Fontana and Staehle, eds. Plenum Press, 1970.

23. Thomas, J. M. and Thomas W. J., "Principles of Heterogeneous Catalysis", Academic Press, New York.

24. Worzula, F. J. and Robinson, W. H., Phil. Mag. 15, 1967, p. 939, in Haslett, W. H., Environment Sensitive Mechanical Behaviour, Gordon and Breach, Publ., p. 319.

25. Castellan, Physical Chemistry, Addison Weslay, 1966.

26. Bastien, P. and Amiot, P., Compt. rend. 235, 1952, p. 1031.

27. Shuetz and Robertson, W. D., Corrosion 13, 1957, p. 631t.

29. Smialowski, M., "Hydrogen in Steel", Pergamon Press, London 1962, p. 397.

30. Boucher, B. Le, Fourth Int. Congr. Metal Corrosion, Extended Abstr., p. 145.

31. Duquette, D. J. and Uhlig, H. H., Trans. A. S. M. 62, 1969, p. 839.

32. Duquette, D. J., and Uhlig, H. H., Trans. A. S. M. 61, 1968, p. 449.

33. Bond, D. C. and Marsh, G. A., Corrosion 6, 1950, p. 22.

34. Johnson, H. H., "Proc. Conf. on Fundamental Aspects of Stress Corrosion Cracking", Staehle et al., eds., 1969, p. 439.

35. Li, C. Y., Talda, P. M., and Wei, R. P., Int. J. Fracture Mech. 3, 1969, p. 29.

36. Fowkes, F. M., "Chemistry and Physics of Interfaces I", Butterworths, Washington, in: Vermilyea Corrosion Sci., 1970, p. 379.

37. Healy, T. M., and Fursteneau, D. W., Colloid Sci., 20, 1965, p. 376, in: Vermilyea Corrosion Sci., 1970, p. 379.

38. Bennet, J. A. in "Fatigue-An Interdisciplinary Approach, p. 209, Burke et al., eds. Syracuse Univ. Press, 1964.

39. Norton, F. J., J. Appl. Phys. II, 262 (1940), in Johnson, ibid 34.

40. Frank, R. C., Swets, D. E. and Fry, D. L., Trans. Met. Soc. A. I. M. E. 212, 1958, p. 219, in Johnson, ibid 34.

41. Uhlig, H. H., Corrosion and Corrosion Control, p. 184.

42. Fast, J. D., "Gases in Metals", Academic Press, London, 1965.

43. Zappfe, C. and Sims, C., Trans. A. I. M. E. 145, 1941, pp. 225.

44. Tetelman, A., Fundamental Aspects of Stress Corrosion Cracking, N. A. C. E., Houston, 1966, pp. 446-64.

45. Troiano, A. R., Trans. ASM 52, 1960, p. 54.

46. Petch, N. O., and Stables, P., Nature 169, 1952, p. 842.

47. Williams, D. P. and Nelson, H. G., Metall. Trans. I, 1970, p. 63.

48. Hayward, D. D. and Trupnell, B. M. W., in "Chemisorption", 2nd ed., Butterworths, London, pp. 236-237.

49. Spitzig, W. A., Tulda, P. M., and Wei, R. P., J. Engry. Fracture Mech. I, 1968, p. 155.

50. CRC Handbook.

51. Grosskreutz, J. C. and Bowles, C. Q., in Haslett, W. H., "Environment Sensitive Mech. Behaviour", Gordon and Breach, New York.

52. Snape, E., Corrosion 24, (9), 1968, p. 261.

53. Bastien, R. G., "Physical Metallurgy of Stress Corrosion Fracture", A. I. M. E., Rhodin, T. N., ed., 1959, p. 311.

54. Ryder, D. A., "The Elements of Fractography", AGARDograph, Advisory Group for Aerospace Research and Development, N. A. T. O.

55. Electron Fractography, ASTM STP 436, Amer. Soc. Testing and Materials, 1968.

TABLES

TABLE I

CHEMICAL COMPOSITIONS & MECHANICAL PROPERTIES
OF
A. P. I. GRADE D 1536 MD STEEL

C	0.36 %
P	0.027
S	0.037
Mn	1.25
Si	0.26
Cu	0.16
Cr	0.15
Ni	0.11
Mo	<0.05
V	0.055
Nb	<0.01

yield strength = 111,000 psi

ultimate strength = 117,000 psi

TABLE 4

FATIGUE TEST DATA

Test	Environment	Stress (psi)	Cycles to Failure	
1-3	Humid H_2S	102,000	1,700	
2-6	"	68,000	3,800	
3-7	"	96,200	600	
4-10	"	84,000	1,900	
5-28	"	89,200	2,500	
6-29	"	75,200	5,500	
7-30	"	57,900	29,300	
8-18	Dry H_2S	77,100	6,600	
9-31	"	93,700	2,500	
10-32	"	62,500	52,500	
11-19	Dry H_2	80,000	10,300	
12-20	"	85,700	10,600	
13-21	"	93,800	4,700	
14-22	"	58,800	58,000	DNF*
15-27	"	70,900	40,000	
16-5	Air	65,000	27,900	
17-8	"	95,600	5,100	
18-9	"	84,300	12,700	
19-17	"	110,000	4,100	
20-11	Dry Argon	93,200	9,200	
21-12	"	80,400	17,900	
22-13	"	65,100	59,500	
23-14	Humid Argon	80,000	17,300	
24-15	"	74,600	7,450	
25-16	"	71,000	33,000	
26-33	"	95,300	9,000	
26-23	Humid H_2	96,800	11,600	
27-24	"	83,800	21,600	
28-25	"	59,400	58,200	DNF*
29-26	"	70,200	53,500	

* Did not fail

FIGURES

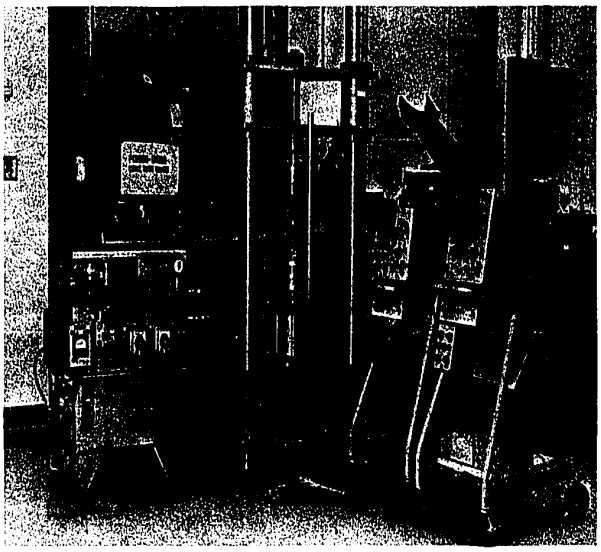

FIGURE 1 FATIGUE TESTING SYSTEM

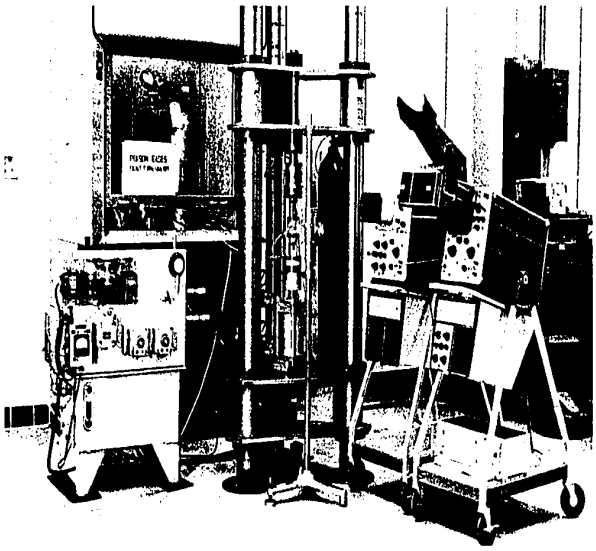

FIGURE 1 FATIGUE TESTING SYSTEM

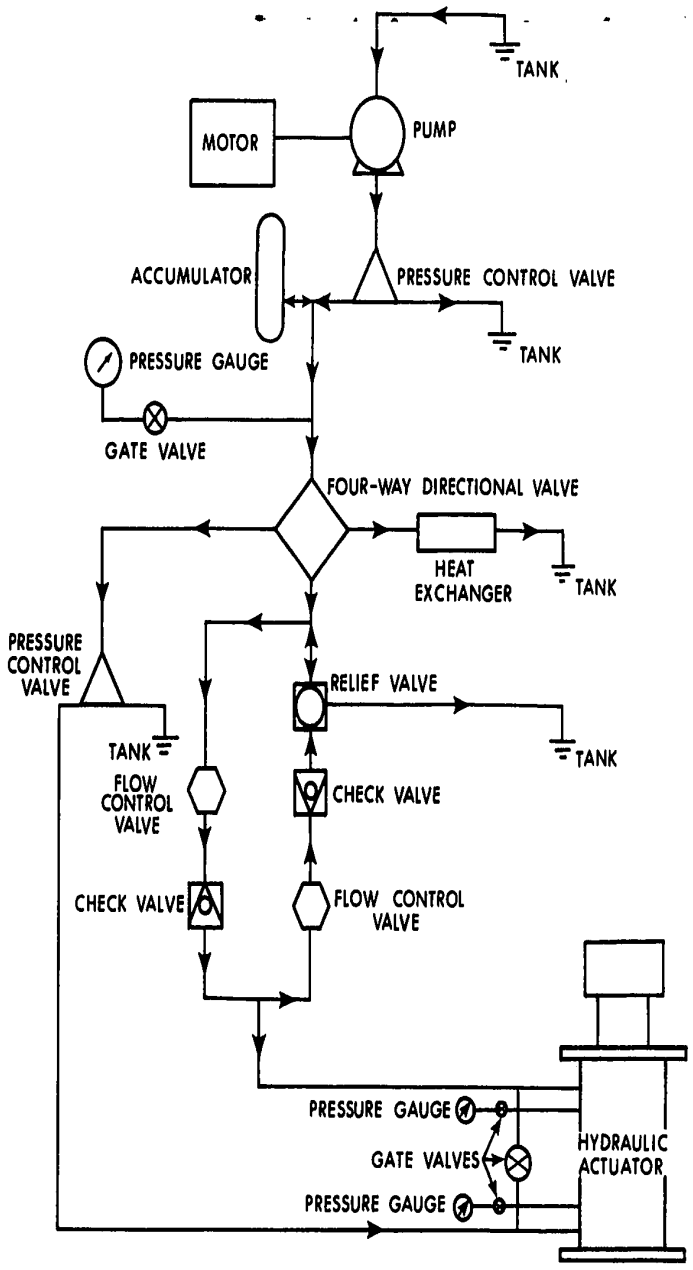

FIGURE 2: Hydraulic circuit showing the pattern of oil flow.

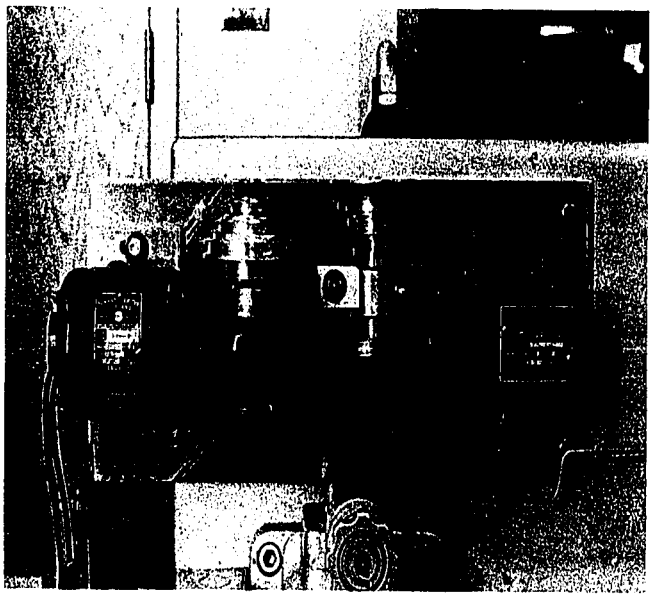

FIGURE 3: Hydraulic cyclic mechanism including motor, belt drive, cam and four-way flow control valve.

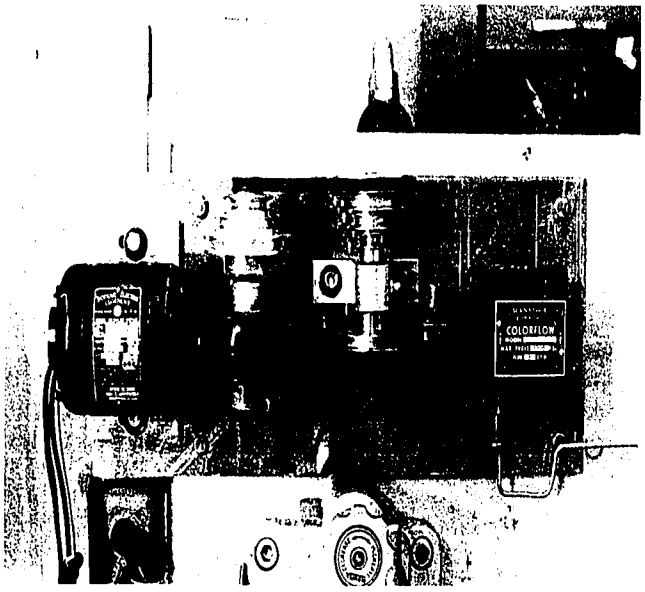

FIGURE 3: Hydraulic cyclic mechanism including motor, belt drive, cam and four-way flow control valve.

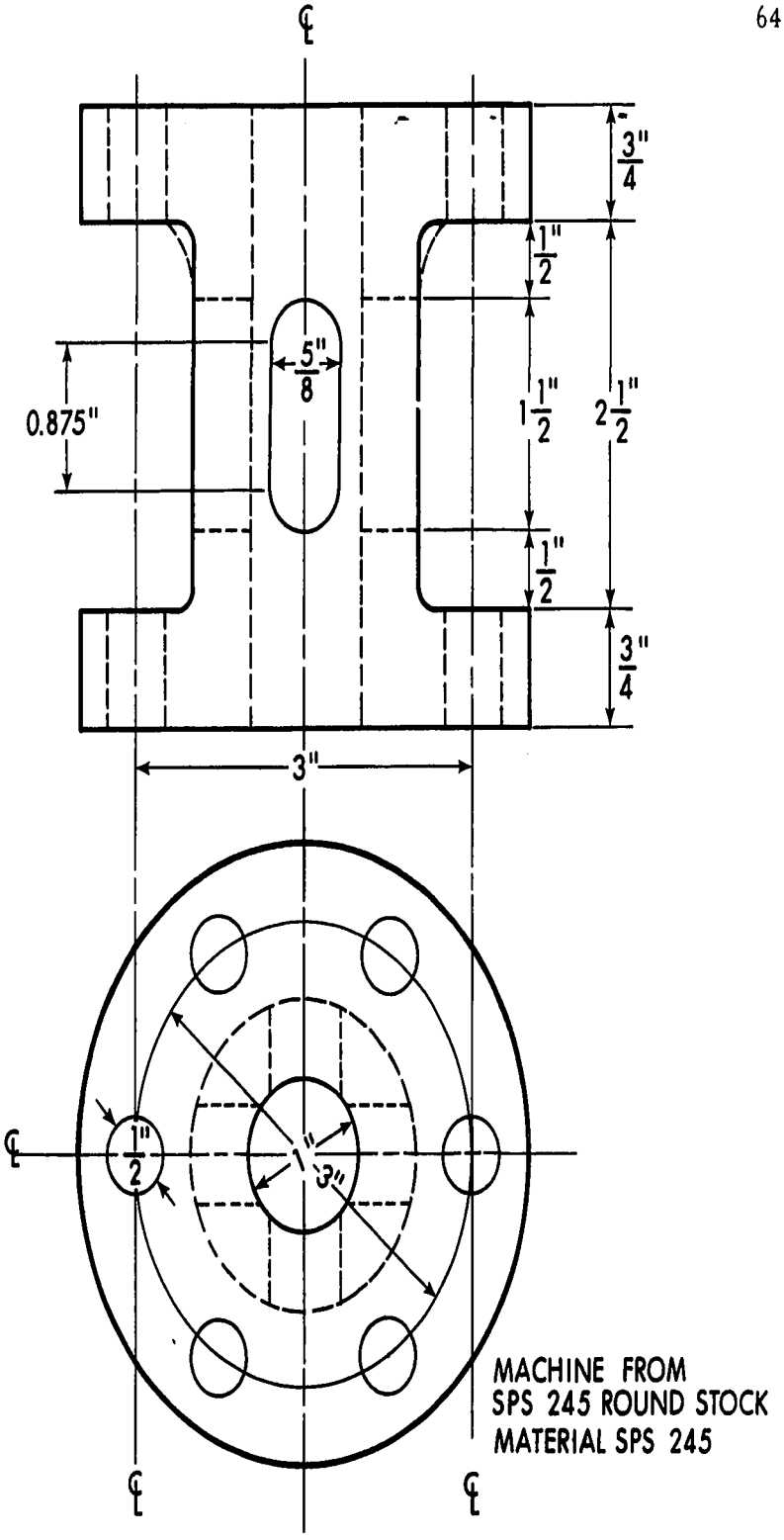

FIGURE 4: Schematic diagram of the load cell.

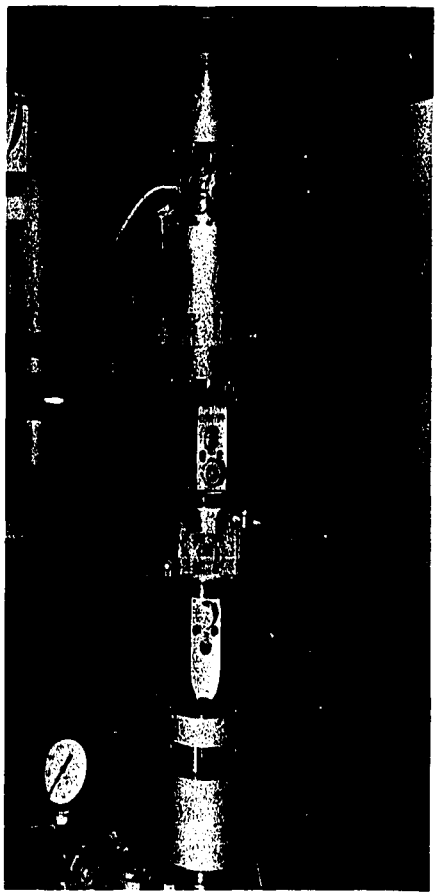

FIGURE 5: Gripping system with environment chamber, load cell and grips.

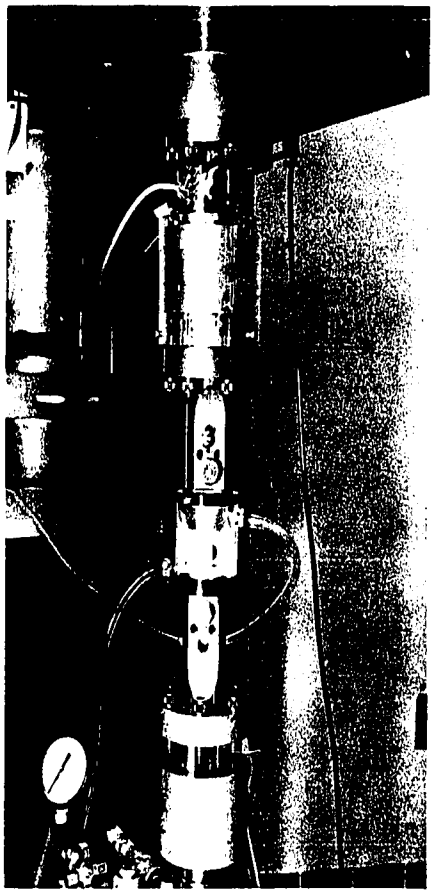

FIGURE 5: Gripping system with environment chamber, load cell and grips.

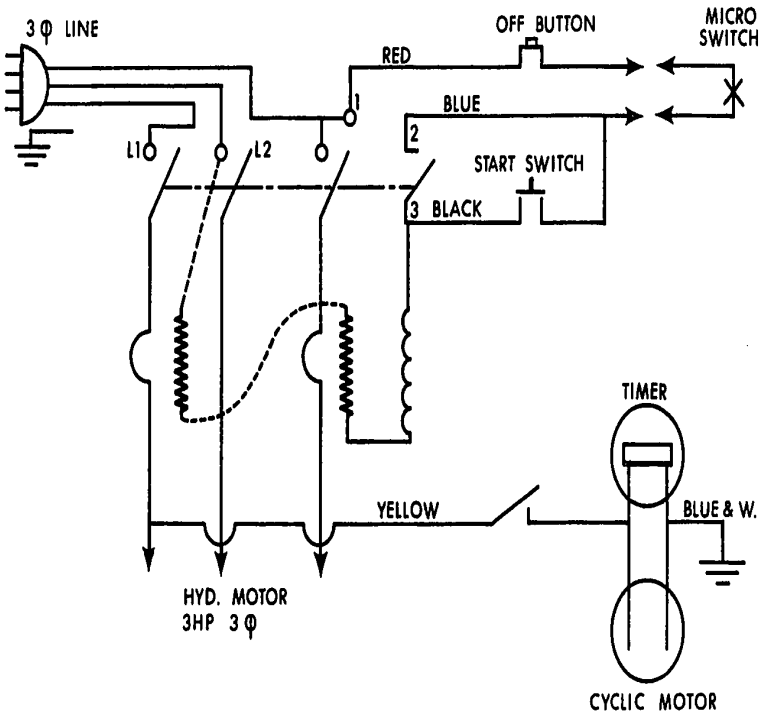

FIGURE 6: Electrical circuit diagram of the fatigue testing system.

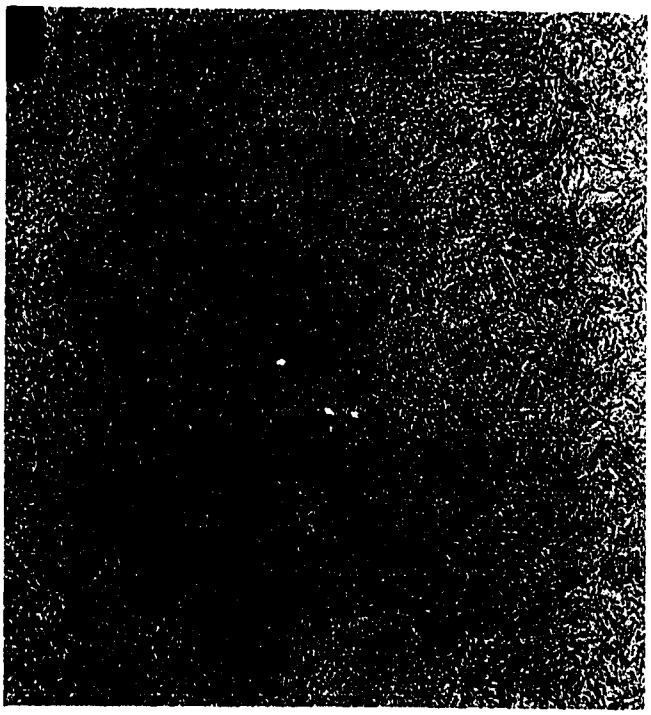

FIGURE 7: Microstructure of the API Grade D 1536 MD steel used in this testing program X 600.

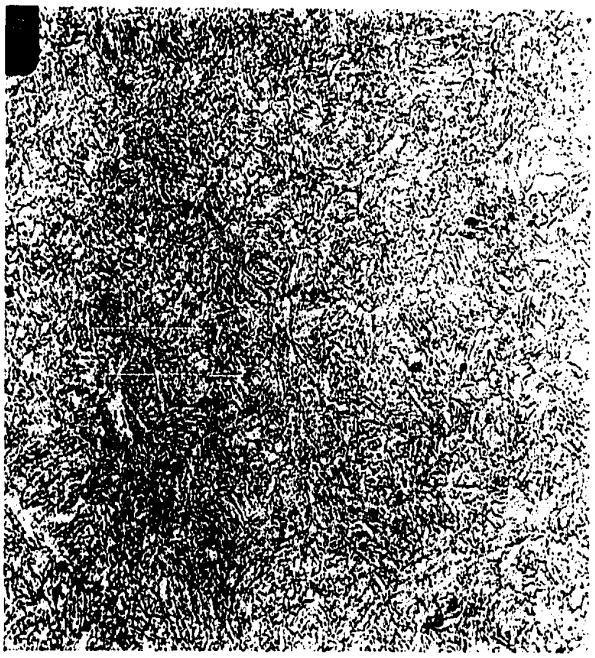

FIGURE 7: Microstructure of the API Grade D 1536 MD steel used in this testing program X 600.

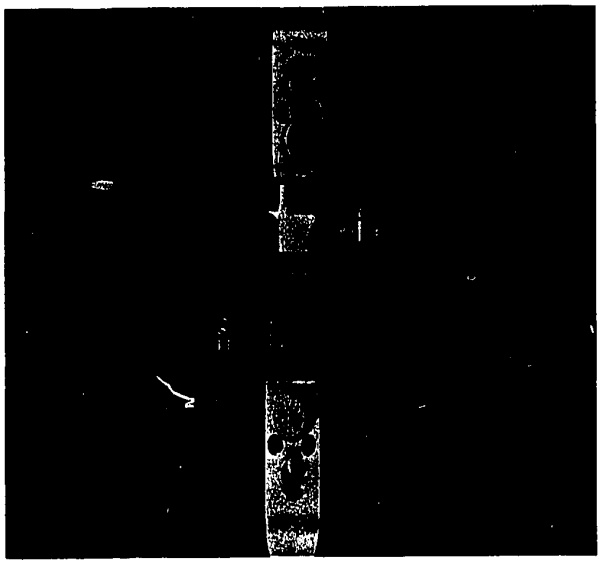

FIGURE 9: ENVIRONMENT CHAMBER

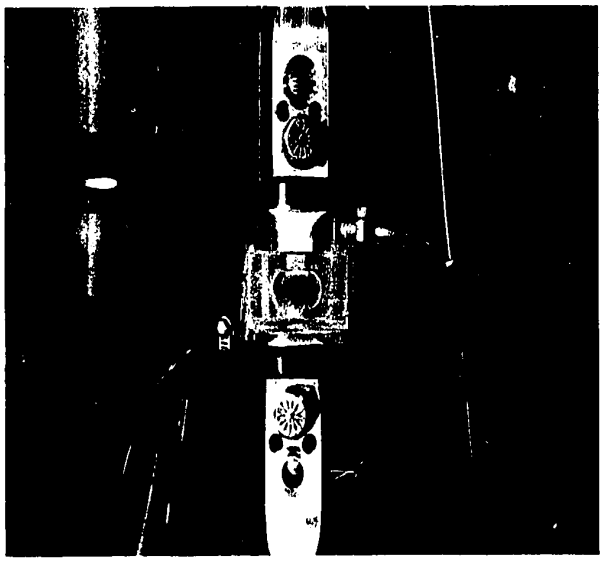

FIGURE 9: ENVIRONMENT CHAMBER

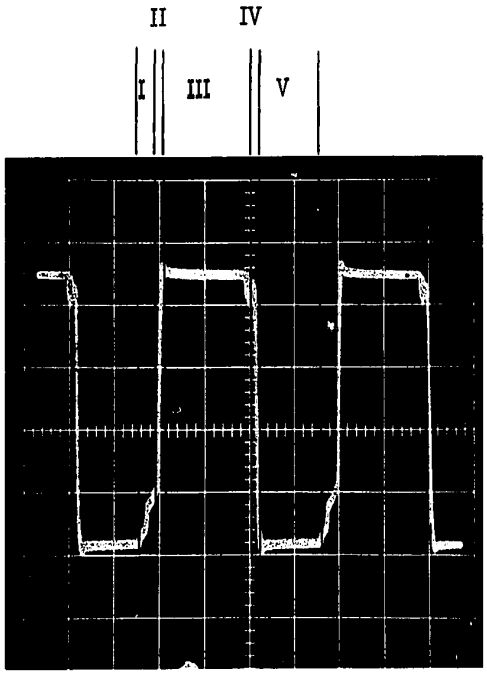

FIGURE 10: Oscilloscope photograph of load versus time. The stages of loading are:

I - increasing loading rate
II - constant loading rate
III - constant load
IV - decreasing load
V - zero load

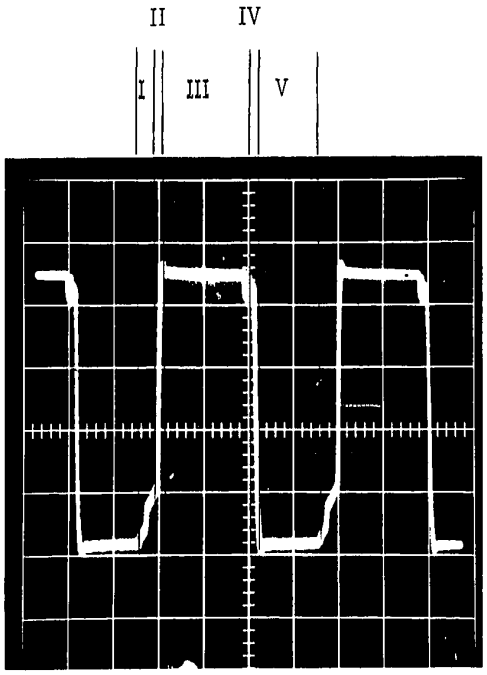

FIGURE 10: Oscilloscope photograph of load versus time. The stages of loading are:

I - increasing loading rate
II - constant loading rate
III - constant load
IV - decreasing load
V - zero load

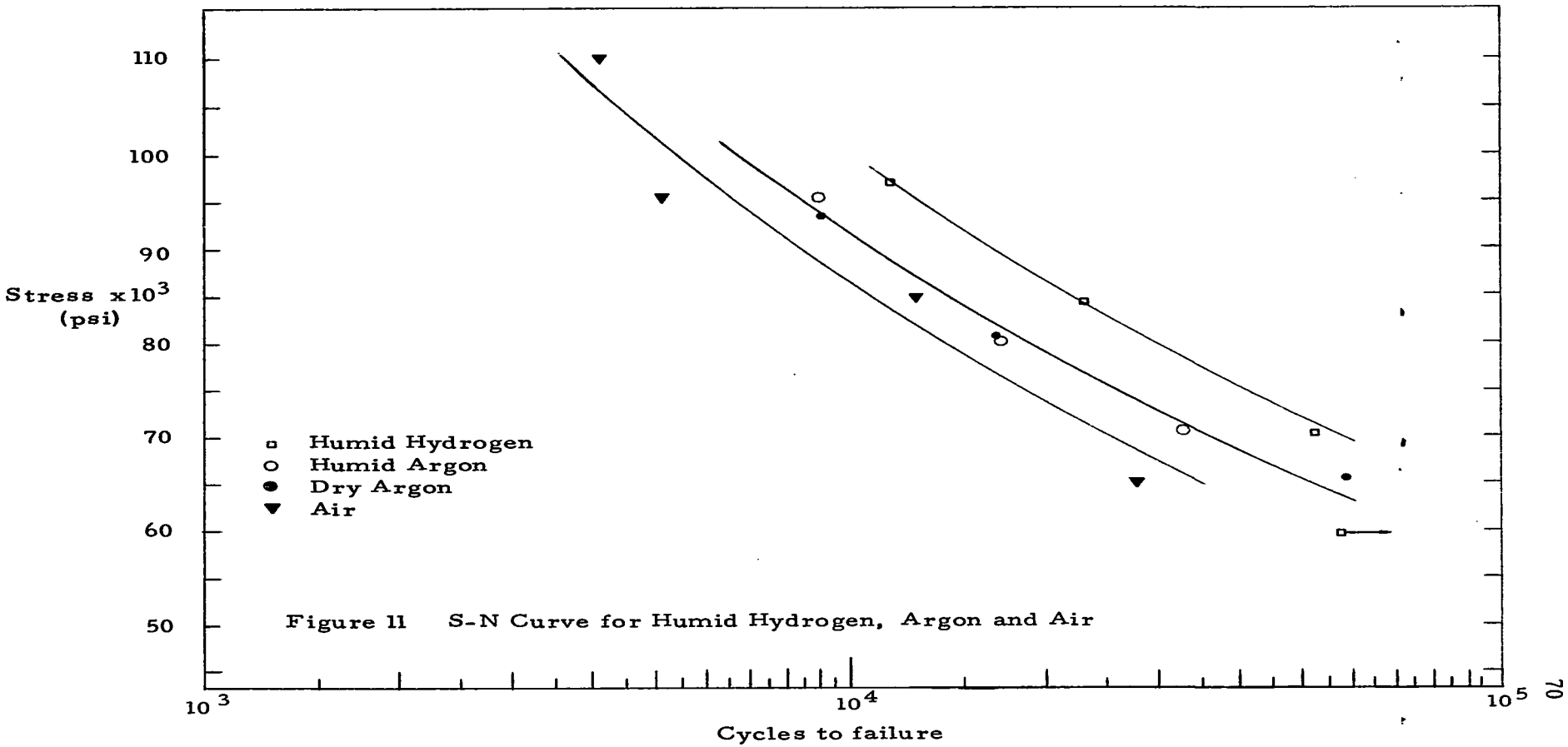

Figure 11 S-N Curve for Humid Hydrogen, Argon and Air

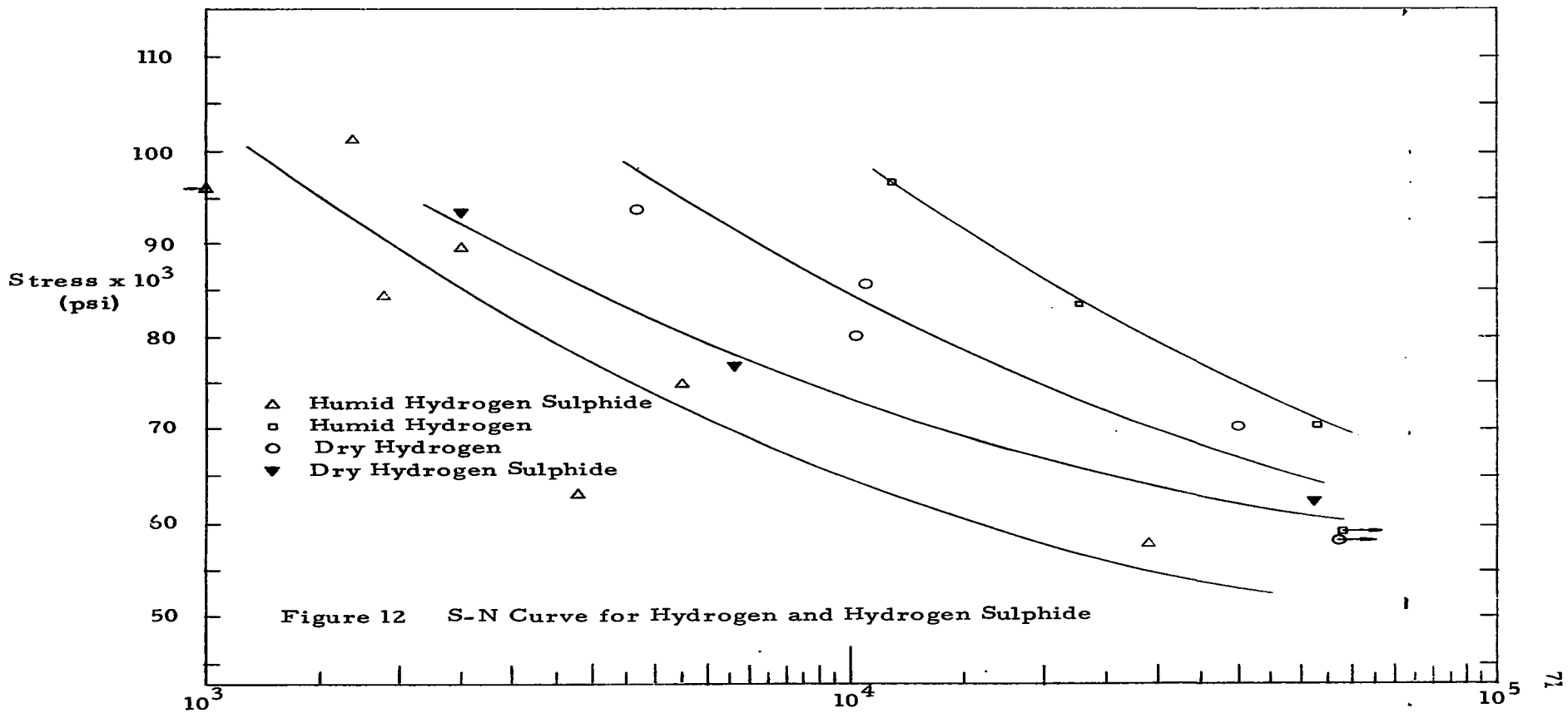

Figure 12 S-N Curve for Hydrogen and Hydrogen Sulphide

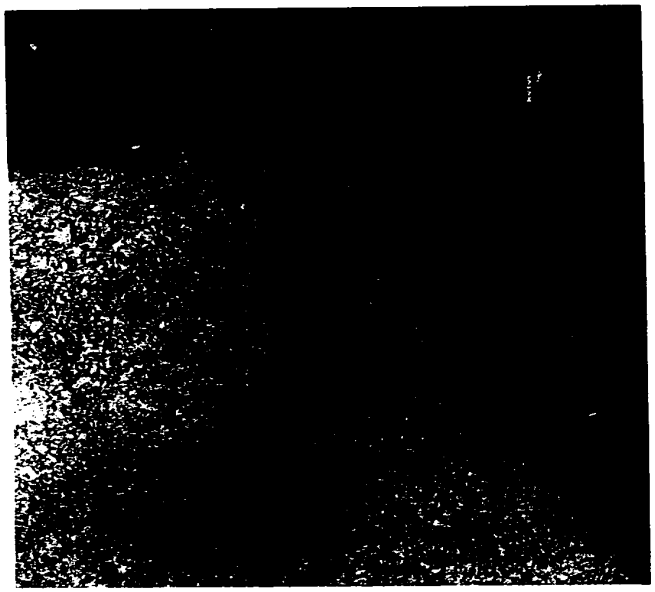

FIGURE 13: Surface crack and branching in humid argon: applied stress = 80,000 psi. X 750

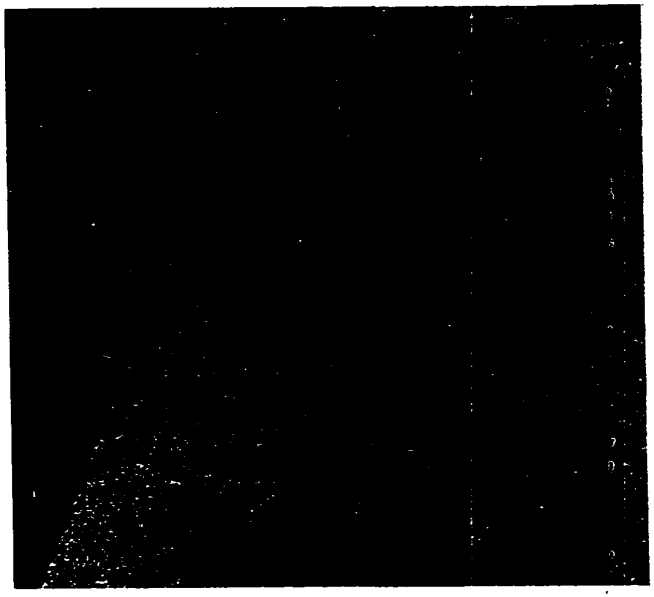

FIGURE 14: Surface crack in humid hydrogen: applied stress = 83,800 psi. X 400

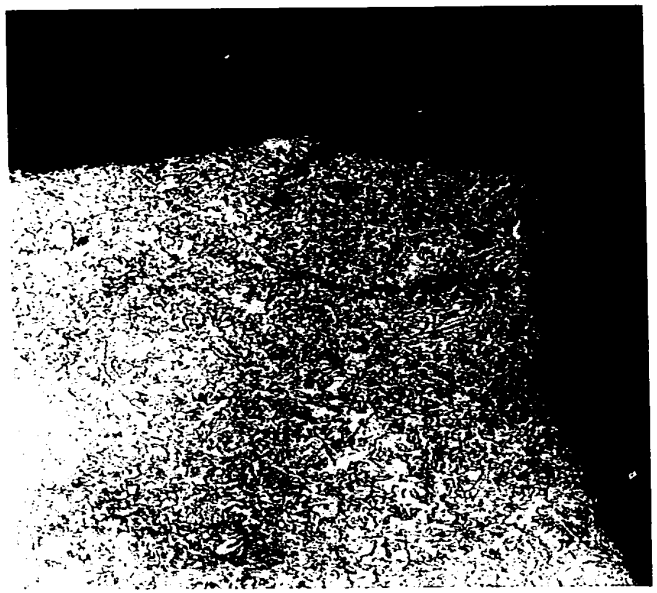

FIGURE 13: Surface crack and branching in humid argon: applied stress = 80,000 psi. X 750

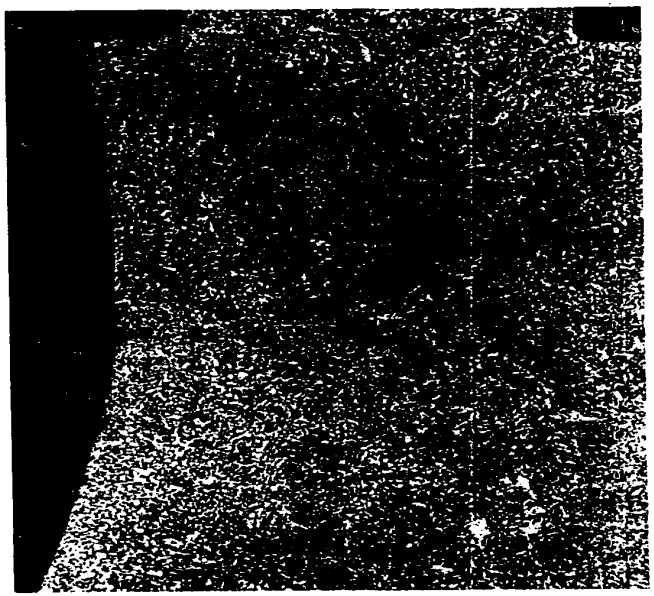

FIGURE 14: Surface crack in humid hydrogen: applied stress = 83,800 psi. X 400

FIGURE 15: Tiny spherules of corrosion product of H_2S corrosion reaction (note flat fracture surfaces).

FIGURE 15: Tiny spherules of corrosion product of H_2S corrosion reaction (note flat fracture surfaces).

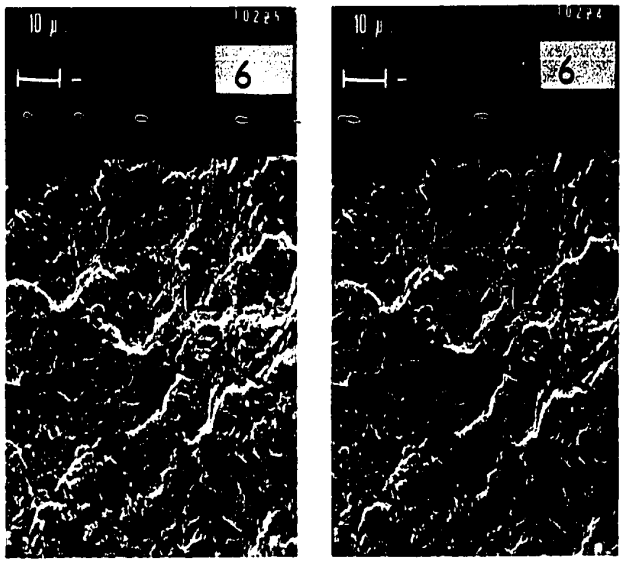

FIGURE 16: Fracture surfaces produced in hydrogen sulphide: stress = 68,000 psi. Same as Fig. 15 (stereo pair) Humid atmosphere.

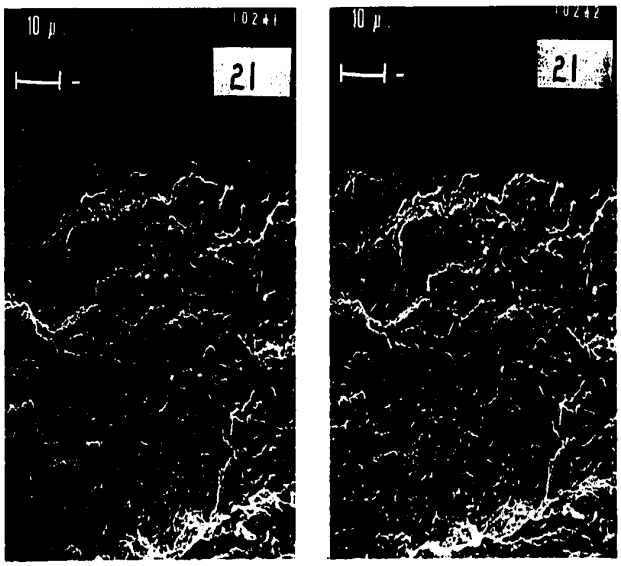

FIGURE 17: Fracture surfaces produced in dry hydrogen: stress = 93,800 psi (stereo pair)

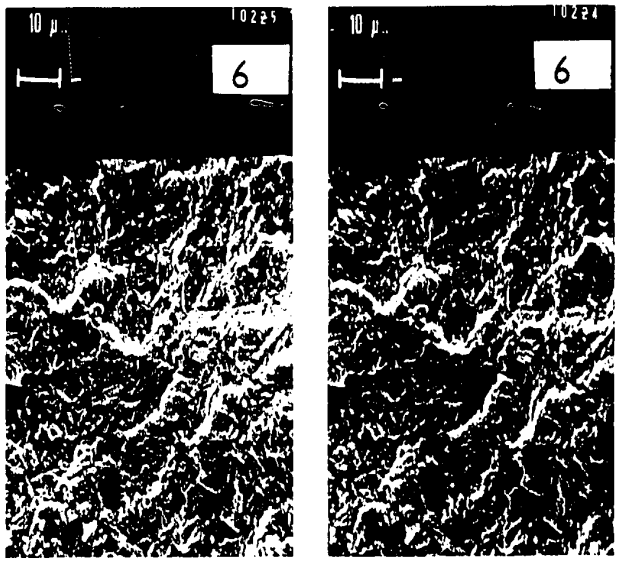

FIGURE 16: Fracture surfaces produced in hydrogen sulphide: stress = 68,000 psi. Same as Fig. 15 (stereo pair) Humid atmosphere.

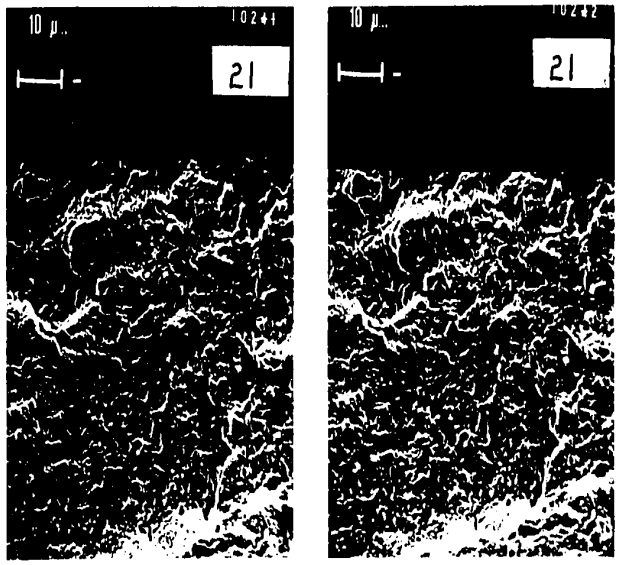

FIGURE 17: Fracture surfaces produced in dry hydrogen: stress = 93,800 psi (stereo pair)

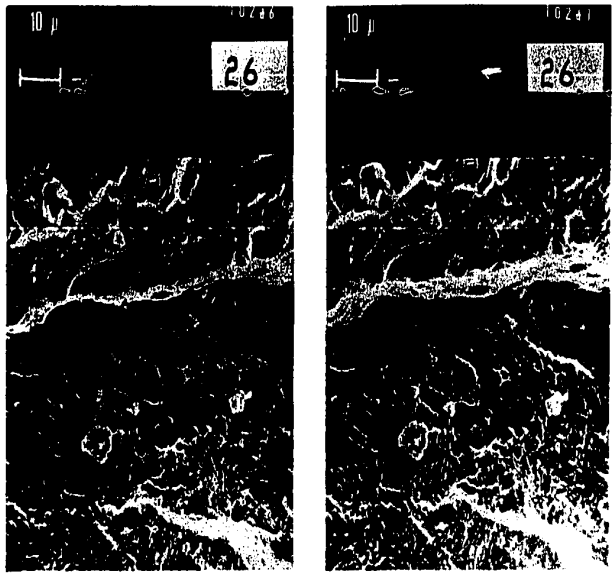

FIGURE 18: Fracture surface produced in humid hydrogen: stress = 95,300 psi (stereo pair)

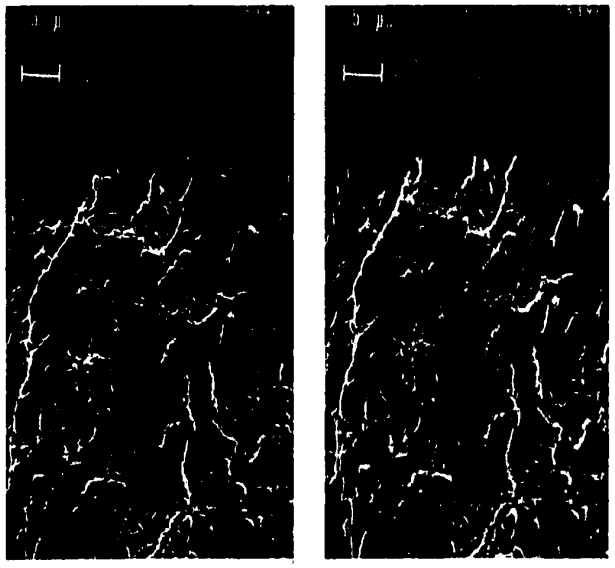

FIGURE 19: Fracture surface produced in dry argon: stress = 83,800 psi (stereo pair)

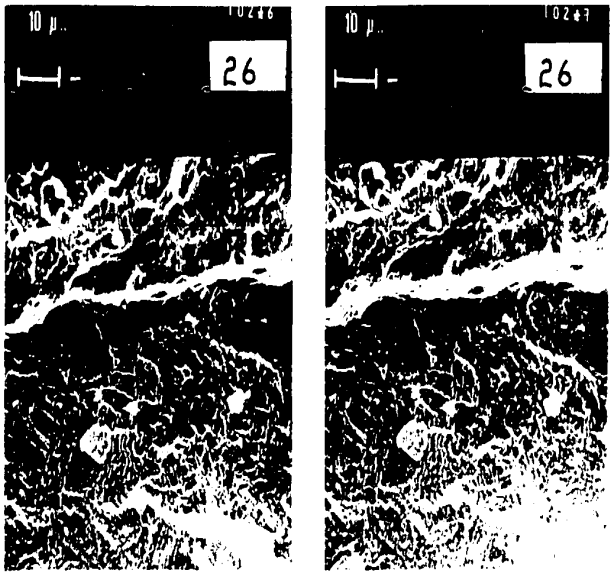

FIGURE 18: Fracture surface produced in humid hydrogen: stress = 95,300 psi (stereo pair)

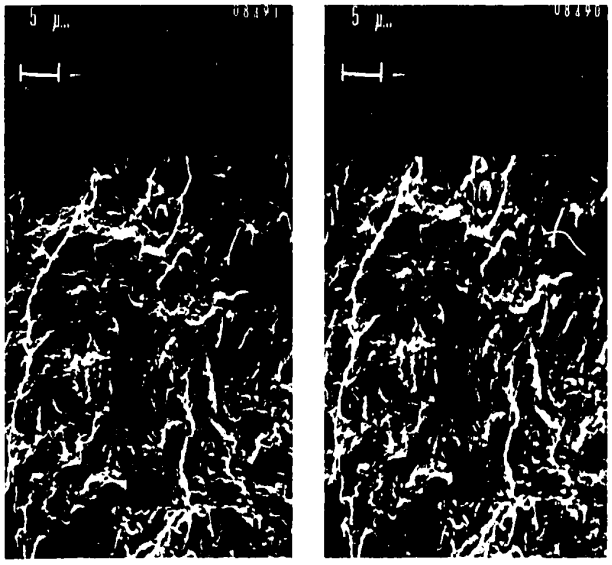

FIGURE 19: Fracture surface produced in dry argon: stress = 83,800 psi (stereo pair)

APPENDIX

APPENDIX A

REACTION OF MOIST HYDROGEN SULPHIDE WITH IRON

A detailed study of the hydrogen sulphide electrochemical corrosion reaction presented has been done by S. P. Ewing, taking into account variables such as CO_2 content, pH, etc.

One litre of water at s. t. p. dissolves about 4. 6 litres of hydrogen sulphide gas. The hydrogen sulphide is weakly ionized in a two step process according to equations 1 and 2.

$$H_2S \longrightarrow HS^- + H^+ \qquad 1$$

$$HS^- \longrightarrow H^+ + S^- \qquad 2$$

The dissociation constants for the above reactions are given in equations 3, 4 and 5.

$$K_1 = \frac{[H^+][HS^-]}{H_2S} = 1.15 \times 10^{-7} \qquad 3$$

$$K_2 = \frac{[H^+][S^=]}{HS^-} = 10^{-15} \qquad 4$$

$$K_1 \cdot K_2 = \frac{[H^+]^2[S^=]}{[H_2S]} = 1.15 \times 10^{-22} \qquad 5$$

where $[H^+]$, $[HS^-]$ $[S^=]$ and $[H_2S]$ represent the respective activity values in solution. When H_2S dissolves in water the pH of the solution drops to about 4.

The reaction of the dissolved hydrogen sulphide with iron in the absence of oxygen is generally considered to follow the reaction:

$$H_2S + Fe \longrightarrow FeS + 2H \qquad 6$$

Equation 6 can be written as the sum of two electrochemical partial reactions occurring at the anode and the cathode.

$$\text{Anode} \quad Fe + S \longrightarrow FeS + 2e^- \qquad 7$$

$$\text{Cathode} \quad 2H^+ + 2e^- \longrightarrow 2H \qquad 8$$

The solubility product for the anodic reaction is low ($[Fe^{++}] \cdot [S^=] \simeq 10^{-19}$) and therefore FeS is precipitated. It is at this point that the effects of pH become important.

At low pH a further reaction occurs (9):

$$FeS + 2H^+ \longrightarrow H_2S + Fe^{++} \qquad 9$$

while in alkaline solutions the activity of the iron ion drops since:

$$[Fe^{++}] \quad \frac{[H^+]2}{10^{-4}} \text{ and } [S^=] \quad \frac{10^{-23}}{[H^+]2} \qquad 10$$

The activities of the iron and sulphur ions are equal at pH = 6. Using this data the precipitation reaction can be explained.

During corrosion, ferrous ions go into solution at anodic areas and diffuse away from the anode. Precipitation of FeS occurs where the solubility product is exceeded. At low pH, the few sulphide ions near the anode are soon precipitated and the zone of precipitation moves out into the solution. On the contrary, in alkaline solutions any ferrous ion p roduced at the anode is immediately precipitated and an adherent layer of FeS is formed. Therefore in solutions of hydrogen sulphide in water the scale is not adherent. The presence

of other dissolved species, such as CO_2, which lower the pH also produce non-adhering scale and the corrosion reaction is not stifled by the corrosion products.

EFFECT OF OXYGEN

Oxygen in solution has the effect of oxidizing the ferous ion to ferric and the sulphide ion to $SO_3^=$ and $SO_4^=$. Depolarization of the cathode may occur according to equations 11 and 12.

$$O_2 + 4H^+ + 4e^- \longrightarrow 2H_2O \qquad 11$$

$$O_2 + 2H_2O + 4e^- \longrightarrow 4OH^-$$

Thus both the anodic and cathodic processes are facilitated and the corrosion rate increases considerably.

ref: Ewing, S. P., Corrosion 12, 1957 pp. 43